# Phenomenological Analysis of Charmless Decays $B \to PV$ with QCD Factorization

Dongsheng Du[a,b], * Haijun Gong[b], † Junfeng Sun[b], ‡ Deshan Yang[b] § and Guohuai Zhu[b,c] **

*a. CCAST (World Laboratory), P.O.Box 8730, Beijing 100080, China*

*b. Institute of High Energy Physics, Chinese Academy of Sciences, P.O.Box 918(4), Beijing 100039, China* ††

*c. Theory Group, KEK, Tsukuba, Ibaraki 305-0801, Japan*

## Abstract

We study hadronic charmless two-body B decays to final states involving pseudoscalar and vector mesons with the QCD factorization approach, including the contributions from the chirally enhanced power corrections and weak annihilations. The CP-averaged branching ratios and CP-violating asymmetries are given. Most of our results are in agreement with the present measurements, but the branching ratios of some decay channels are only marginally consistent with the experimental observations. Considering the large uncertainties, great advances in both experiment and theory in the near future are

*Email address:duds@mail.ihep.ac.cn

†Email address:gonghj@mail.ihep.ac.cn

‡Email address:sunjf@mail.ihep.ac.cn

§Email address:yangds@mail.ihep.ac.cn

**Email address:zhugh@post.kek.jp

††Mailing address

strongly expected.

PACS number(s):13.25.Hw 12.38.Bx

## I. INTRODUCTION

In the standard model (SM), CP violation is described by the phase of the Cabibbo-Kobayashi-Maskawa (CKM) matrix. Phenomenologically, it is clear and convenient to explore CP violation with the well-known unitarity triangle $V_{ud}V_{ub}^* + V_{cd}V_{cb}^* + V_{td}V_{tb}^* = 0$. In a sense, the study of $B$ meson decays is mainly to make enough independent measurements of the sides and angles of this unitarity triangle. It is thus crucial to have a clear understanding of exclusive hadronic charmless B decays which would give some useful information about and/or constraints on the unitarity triangle. Recently, several experimental groups have reported their latest results [1–16], and more B decay channels will be measured with great precision soon. With the accumulation of the experimental data, theorists are urged to gain deep insight into the rare hadronic B decays, and reduce the theoretical uncertainties in determining the CKM parameters from experimental measurements.

Theoretically, intense investigations of hadronic charmless two-body B decays have been carried out in great detail with the effective Hamiltonian. Combining operator product expansion with the renormalization group method, the effective Hamiltonian for B decays is generally expressed by the products of the Wilson coefficients and dimension-6 effective operators. The Wilson coefficients can be calculated reliably by perturbation theory, they have been evaluated to the next-to-leading order [17]. Thus, the main task for us is to evaluate the hadronic matrix elements of the effective operators. Based on the naive factorization (NF) hypothesis [18], which is supported by the argument of color transparency [19], the hadronic matrix elements are usually parametrized into the product of the decay constants and the transition form factors phenomenologically. The NF approach works well for B and D decays, at least it can give the proper orders of magnitude of the branching ratios for B and D decays. However, the NF approach is a very rough approximation, and has obvious shortcomings: (1) In the NF framework, the renormalization scheme- and scale-dependence in the hadronic matrix elements are completely missing. Its predictions would be physical only when the hadronic matrix elements could make compensation for the renormalization

scheme- and scale-dependence of the Wilson coefficients. (2) There is no direct CP violation in hadronic B decays with the NF approach because the Wilson coefficients, decay constants, and form factors are all real. This indicates that "nonfactorizable" contributions, which account for final-state rescattering and the strong interaction phase shift, are important. (3) As stated in [20], it is questionable whether "nonfactorizable" effects can be simply absorbed into decay constants and form factors. They will have great effects on the class II ($a_2$ dominant) decay modes, e.g. $B^0 \to \rho^0\pi^0, \rho^0\eta, \omega\eta, \cdots$. So it is imperative to go beyond this level of understanding.

Recently, M. Beneke, G. Buchalla, M. Neubert, and C. T. Sachrajda suggested a QCD factorization (QCDF) method for hadronic B decays in the heavy quark limit, combining the hard-scattering approach with power counting in $1/m_b$ [21]. The hadronic matrix elements $\langle M_1 M_2|O_i|B\rangle$ (here $M_1$ denotes the recoiled meson which picks up the light spectator quark in the B meson, $M_2$ is the emitted meson, and $O_i$ are effective operators) can be computed from first principles and expressed in terms of form factors and meson light-cone distribution amplitudes (LCDAs) only if $M_2$ is light or an onium. In addition, when $M_1$ is light, there exist hard-scattering interactions between $M_2$ and the spectator which do not exist in the NF approach. The QCDF approach shows that the "nonfactorizable" contributions are dominated by hard gluon exchange and therefore computable systematically. Detailed proofs and arguments can be found in [21]; its applications to hadronic two-body B decays can be found in the literature [21–28].

In recent work [28], we calculated the branching ratios and CP asymmetries for $B \to PP$ (where $P$ denotes the pseudoscalar meson) within the QCDF approach. We found that with appropriate parameters our results are in agreement with the current experimental data. This encouraged us to further investigate the exclusive decays $B \to PV$ (where $V$ denotes the vector meson) with the QCDF method. The $B \to PV$ decays have been carefully studied within generalized factorization [20,29,30], and some decay channels have also been studied with the perturbative QCD approach [31] where the form factors are believed to be perturbatively calculable with the assistance of the Sudakov factors. However, it is still an

open question whether the Sudakov factor is applicable in B meson decays [32]. In the QCDF framework, it is argued [21] that the form factors are not fully calculable according to naive power counting. M. Yang and Y. Yang studied the decay modes $B\to h_1h_2$ ($h_1=\pi,K$ and $h_2=K^*,\rho,\omega$) in [25] using the QCDF approach. The differences between their work and ours are that we consider the chirally enhanced contributions from another type of twist-3 LCDAs $\phi_\sigma$ of the pseudoscalar mesons, which is crucial for gauge independence, and we also take the weak annihilation topologies into account. H. Cheng and K. Yang pointed out that the annihilation contributions could be sizeable for the decays $B\to\phi K$ [24]. Sometimes, the annihilation contributions may even be dominant, e.g., $B^0\to K^\pm K^{*\mp}$. In this paper, we will undertake a comprehensive study of the hadronic charmless decays of $B\to PV$ within the QCDF framework, including the effects of weak annihilation and the chirally enhanced contributions.

This paper is organized as follows. Section II is devoted to the theoretical framework. There we calculate the "nonfactorizable" corrections to hadronic matrix elements of the effective operators with the QCDF approach, including the chirally enhanced power corrections and weak annihilations. The input parameters in our calculations are given in Sec. III. The numerical values and some remarks about the CP-averaged branching ratios and CP-violating asymmetries for $B\to PV$ decays are arranged in Sec. IV and Sec. V, respectively. We come to our final conclusions in Sec. VI.

## II. THEORETICAL FRAMEWORK FOR B DECAYS

### A. The effective Hamiltonian

The effective Hamiltonian for hadronic charmless B decays is written as [17]:

$$\begin{aligned}\mathcal{H}_{eff}=\frac{G_F}{\sqrt{2}}\Big\{\sum_{q=u,c}v_q\Big[C_1(\mu)Q_1^q(\mu)+C_2(\mu)Q_2^q(\mu)+\sum_{k=3}^{10}C_k(\mu)Q_k(\mu)\Big]\\ -v_t\Big[C_{7\gamma}Q_{7\gamma}+C_{8g}Q_{8g}\Big]\Big\}+H.c.,\end{aligned}\tag{2.1}$$

where $v_q = V_{qb}V_{qd}^*$ (for $b\to d$ transitions) or $v_q = V_{qb}V_{qs}^*$ (for $b\to s$ transitions) are CKM factors. $C_i(\mu)$ are Wilson coefficients; they are universal and process independent, and have been evaluated to the next-to-leading logarithmic order (NLO) with the perturbation theory and renormalization group method. We list their numerical values in the naive dimensional regularization (NDR) scheme at three different scales in Table I. The dimension-6 local operators, including tree operators $Q_1^q{\sim}Q_2^q$, QCD penguin operators $Q_3{\sim}Q_6$, electroweak penguin operators $Q_7{\sim}Q_{10}$, and magnetic penguin operators $Q_{7\gamma}, Q_{8g}$, can be expressed explicitly as

$$Q_1^u = (\bar{u}_\alpha b_\alpha)_{V-A}(\bar{q}_\beta u_\beta)_{V-A}, \qquad Q_1^c = (\bar{c}_\alpha b_\alpha)_{V-A}(\bar{q}_\beta c_\beta)_{V-A}, \tag{2.2a}$$

$$Q_2^u = (\bar{u}_\alpha b_\beta)_{V-A}(\bar{q}_\beta u_\alpha)_{V-A}, \qquad Q_2^c = (\bar{c}_\alpha b_\beta)_{V-A}(\bar{q}_\beta c_\alpha)_{V-A}, \tag{2.2b}$$

$$Q_3 = (\bar{q}_\alpha b_\alpha)_{V-A}\sum_{q'}(\bar{q}'_\beta q'_\beta)_{V-A}, \qquad Q_4 = (\bar{q}_\beta b_\alpha)_{V-A}\sum_{q'}(\bar{q}'_\alpha q'_\beta)_{V-A}, \tag{2.2c}$$

$$Q_5 = (\bar{q}_\alpha b_\alpha)_{V-A}\sum_{q'}(\bar{q}'_\beta q'_\beta)_{V+A}, \qquad Q_6 = (\bar{q}_\beta b_\alpha)_{V-A}\sum_{q'}(\bar{q}'_\alpha q'_\beta)_{V+A}, \tag{2.2d}$$

$$Q_7 = \frac{3}{2}(\bar{q}_\alpha b_\alpha)_{V-A}\sum_{q'} e_{q'}(\bar{q}'_\beta q'_\beta)_{V+A}, \qquad Q_8 = \frac{3}{2}(\bar{q}_\beta b_\alpha)_{V-A}\sum_{q'} e_{q'}(\bar{q}'_\alpha q'_\beta)_{V+A}, \tag{2.2e}$$

$$Q_9 = \frac{3}{2}(\bar{q}_\alpha b_\alpha)_{V-A}\sum_{q'} e_{q'}(\bar{q}'_\beta q'_\beta)_{V-A}, \qquad Q_{10} = \frac{3}{2}(\bar{q}_\beta b_\alpha)_{V-A}\sum_{q'} e_{q'}(\bar{q}'_\alpha q'_\beta)_{V-A}, \tag{2.2f}$$

$$Q_{7\gamma} = \frac{e}{8\pi^2} m_b \bar{q}_\alpha \sigma^{\mu\nu}(1+\gamma_5) b_\alpha F_{\mu\nu}, \qquad Q_{8g} = \frac{g}{8\pi^2} m_b \bar{q}_\alpha \sigma^{\mu\nu}(1+\gamma_5) t^a_{\alpha\beta} b_\beta G^a_{\mu\nu}, \tag{2.2g}$$

where $q'$ denotes all the active quarks at the scale $\mu = \mathcal{O}(m_b)$, i.e., $q' = u, d, s, c, b$.

### B. $B\to PV$ in the QCDF framework

When the QCDF method is applied to the decays $B\to PV$, the hadronic matrix elements of the local effective operators can be written as

$$\begin{aligned}\langle PV|O_i|B\rangle = {} & F_j^{B\to P}(0)\int_0^1 dx\; T_{ij}^I(x)\Phi_V(x) + A_k^{B\to V}(0)\int_0^1 dy\; T_{ik}^I(y)\Phi_P(y) \\ & + \int_0^1 d\xi \int_0^1 dx \int_0^1 dy\; T_i^{II}(\xi, x, y)\Phi_B(\xi)\Phi_V(x)\Phi_P(y).\end{aligned} \tag{2.3}$$

Here $F^{B\to P}$ and $A^{B\to V}$ denote the form factors for $B\to P$ and $B\to V$ transitions, respectively. $\Phi_B(\xi)$, $\Phi_V(x)$, and $\Phi_P(y)$ are the LCDAs of valence quark Fock states for B, vector, and

pseudoscalar mesons, respectively. $T_i^{I,II}$ denote the hard-scattering kernels, which are dominated by hard gluon exchange when the power suppressed $\mathcal{O}(\Lambda_{QCD}/m_b)$ terms are neglected. So they are calculable order by order in perturbation theory. The leading terms of $T^I$ come from the tree level and correspond to the NF approximation. The order of $\alpha_s$ terms of $T^I$ can be depicted by vertex-correction diagrams Fig.1(a-d) and penguin-correction diagrams Fig.1(e-f). $T^{II}$ describes the hard interactions between the spectator quark and the emitted meson $M_2$ when the gluon virtuality is large. Its lowest order terms are $\mathcal{O}(\alpha_s)$ and can be depicted by hard spectator scattering diagrams Fig.1(g-h). One of the most interesting results of the QCDF approach is that, in the heavy quark limit, the strong phases arise naturally from the hard-scattering kernels at the order of $\alpha_s$. As for the nonperturbative part, it is either power suppressed in $1/m_b$ or separated into the form factors and LCDAs of mesons.

Because the b quark mass is not asymptotically large, the power suppression might fail in some cases. For instance, the contributions of operator $Q_6$ to the decay amplitudes would formally vanish in the strict heavy quark limit. However, it is numerically very important in penguin-dominated B rare decays, such as the interesting channels $B\to\pi K$, etc. This is because $Q_6$ is always multiplied by a formally power suppressed but chirally enhanced factor $r_\chi = \frac{2m_P^2}{m_b(m_1+m_2)} \sim \mathcal{O}(1)$, where $m_1$ and $m_2$ are current quark masses. Therefore phenomenological application of QCD factorization in B rare decays requires at least a consistent inclusion of chirally enhanced corrections. The readers may refer to Refs. [22,27] for more details.

With the above discussions on the effective Hamiltonian of B decays Eq.(2.1) and the QCDF expressions of hadronic matrix elements Eq.(2.3), the decay amplitudes for $B\to PV$ in the heavy quark limit can be written as

$$\mathcal{A}(B\to PV) = \frac{G_F}{\sqrt{2}} \sum_{p=u,c} \sum_{i=1}^{10} v_p a_i^p \langle PV|O_i|B\rangle_f. \tag{2.4}$$

The above $\langle PV|O_i|B\rangle_f$ are the factorized hadronic matrix elements, which have the same definitions as those in the NF approach. The "nonfactorizable" effects are included in the

coefficients $a_i$ which are process dependent. The coefficients $a_i$ are collected in Sec. II C, and the explicit expressions for the decay amplitudes of $B\to PV$ can be found in Appendix.B of [29]. The only differences from ours are the expressions for the coefficients $a_i$.

According to the arguments in [21], the contributions of weak annihilation to the decay amplitudes are power suppressed, and they do not appear in the QCDF formula Eq.(2.3). But, as emphasized in [34,35], the contributions from weak annihilation could give large strong phases with QCD corrections, and hence large CP violation could be expected, so their effects cannot simply be neglected. However, in the QCDF method, the annihilation topologies (see Fig.2) violate factorization because of the endpoint divergence. There is similar endpoint divergence when considering the chirally enhanced hard spectator scattering. One possible way is to treat the endpoint divergence from different sources as different phenomenological parameters [22]. The corresponding price is the introduction of model dependence and extra numerical uncertainties in the decay amplitudes. In this work, we will follow the treatment of Ref. [22] and express the weak annihilation topological decay amplitudes as

$$\mathcal{A}^a(B\to PV)\propto f_B f_P f_V \sum v_p b_i \ , \tag{2.5}$$

where the parameters $b_i$ are collected in Sec. II D, and the expressions for the weak annihilation decay amplitudes of $B\to PV$ are listed in the Appendix A. To distinguish the decay amplitudes Eq.(2.4) from Eq.(2.5), we will add a superscript $f$ to the symbol in Eq.(2.4), and write it as $\mathcal{A}(B\to PV)\to\mathcal{A}^f(B\to PV)$.

### C. The QCD coefficients $a_i$

We now present the QCD coefficients $a_i$ in Eq.(2.4). In our calculations, we neglect the mass of light quarks when we apply the equation of motion to the external quarks. We consider the chirally enhanced contributions from twist-3 LCDAs of the pseudoscalar mesons. As for the vector mesons, only the leading twist LCDAs for the longitudinally

polarized components $\Phi_V^{\parallel}$ contribute to the hadronic matrix elements, while the effects of twist-2 LCDAs for the transversely polarized components $\Phi_V^{\perp}$ and higher twist LCDAs of the vector mesons are power suppressed and can therefore be neglected within the QCDF framework. We express the coefficients $a_i$ in two parts, i.e., $a_i = a_{i,I} + a_{i,II}$. The first term $a_{i,I}$ contains the "nonfactorizable" effects which are described by Fig.1(a-f), while the second part $a_{i,II}$ corresponds to the hard spectator scattering diagrams Fig.1(g-h).

There are two different cases according to the final states. Case I is that the recoiled meson $M_1$ is a vector meson, and the emitted meson $M_2$ corresponds to a pseudoscalar meson, and vice versa for case II. For case I, we sum up the results for $a_i$ as follows:

$$a_{1,I} = C_1 + \frac{C_2}{N_c}\Big[1 + \frac{C_F\alpha_s}{4\pi}V_M\Big], \qquad a_{1,II} = \frac{\pi C_F\alpha_s}{N_c^2}C_2 H(BM_1, M_2), \tag{2.6a}$$

$$a_{2,I} = C_2 + \frac{C_1}{N_c}\Big[1 + \frac{C_F\alpha_s}{4\pi}V_M\Big], \qquad a_{2,II} = \frac{\pi C_F\alpha_s}{N_c^2}C_1 H(BM_1, M_2), \tag{2.6b}$$

$$a_{3,I} = C_3 + \frac{C_4}{N_c}\Big[1 + \frac{C_F\alpha_s}{4\pi}V_M\Big], \qquad a_{3,II} = \frac{\pi C_F\alpha_s}{N_c^2}C_4 H(BM_1, M_2), \tag{2.6c}$$

$$a_{4,I}^p = C_4 + \frac{C_3}{N_c}\Big[1 + \frac{C_F\alpha_s}{4\pi}V_M\Big] + \frac{C_F\alpha_s}{4\pi}\frac{P_{M,2}^p}{N_c}, \qquad a_{4,II} = \frac{\pi C_F\alpha_s}{N_c^2}C_3 H(BM_1, M_2), \tag{2.6d}$$

$$a_{5,I} = C_5 + \frac{C_6}{N_c}\Big[1 - \frac{C_F\alpha_s}{4\pi}V_M'\Big], \qquad a_{5,II} = -\frac{\pi C_F\alpha_s}{N_c^2}C_6 H'(BM_1, M_2), \tag{2.6e}$$

$$a_{6,I}^p = C_6 + \frac{C_5}{N_c}\Big[1 - 6\frac{C_F\alpha_s}{4\pi}\Big] + \frac{C_F\alpha_s}{4\pi}\frac{P_{M,3}^p}{N_c}, \qquad a_{6,II} = 0, \tag{2.6f}$$

$$a_{7,I} = C_7 + \frac{C_8}{N_c}\Big[1 - \frac{C_F\alpha_s}{4\pi}V_M'\Big], \qquad a_{7,II} = -\frac{\pi C_F\alpha_s}{N_c^2}C_8 H'(BM_1, M_2), \tag{2.6g}$$

$$a_{8,I}^p = C_8 + \frac{C_7}{N_c}\Big[1 - 6\frac{C_F\alpha_s}{4\pi}\Big] + \frac{\alpha}{9\pi}\frac{P_{M,3}^{p,ew}}{N_c}, \qquad a_{8,II} = 0, \tag{2.6h}$$

$$a_{9,I} = C_9 + \frac{C_{10}}{N_c}\Big[1 + \frac{C_F\alpha_s}{4\pi}V_M\Big], \qquad a_{9,II} = \frac{\pi C_F\alpha_s}{N_c^2}C_{10} H(BM_1, M_2), \tag{2.6i}$$

$$a_{10,I}^p = C_{10} + \frac{C_9}{N_c}\Big[1 + \frac{C_F\alpha_s}{4\pi}V_M\Big] + \frac{\alpha}{9\pi}\frac{P_{M,2}^{p,ew}}{N_c}, \qquad a_{10,II} = \frac{\pi C_F\alpha_s}{N_c^2}C_9 H(BM_1, M_2), \tag{2.6j}$$

where $C_F = \frac{N_c^2-1}{2N_c}$, and $N_c = 3$. The vertex parameters $V_M$ and $V_M'$ result from Fig.1(a-d); the QCD penguin parameters $P_{M,i}^p$ and the electroweak penguin parameters $P_{M,i}^{p,ew}$ result from Fig.1(e-f). The expressions for the penguin parameters are a little different from those in [22]. Here we consider the corrections of the electroweak penguins to $P_{M,i}^p$, and the contributions of the QCD penguins to $P_{M,i}^{p,ew}$. They can be written as

$$P^p_{M,2} = C_1\Big[\frac{4}{3}\ln\frac{m_b}{\mu} + \frac{2}{3} - G_M(s_p)\Big] + \Big(C_3 - \frac{1}{2}C_9\Big)\Big[\frac{8}{3}\ln\frac{m_b}{\mu} + \frac{4}{3} - G_M(0) - G_M(1)\Big]$$
$$+ \sum_{q=q'}\Big(C_4 + C_6 + \frac{3}{2}e_qC_8 + \frac{3}{2}e_qC_{10}\Big)\Big[\frac{4}{3}\ln\frac{m_b}{\mu} - G_M(s_q)\Big]$$
$$-2C_{8g}\int_0^1 dx\ \frac{\Phi_M(x)}{1-x}, \tag{2.7a}$$

$$P^p_{M,3} = C_1\Big[\frac{4}{3}\ln\frac{m_b}{\mu} + \frac{2}{3} - \hat{G}_M(s_p)\Big] + \Big(C_3 - \frac{1}{2}C_9\Big)\Big[\frac{8}{3}\ln\frac{m_b}{\mu} + \frac{4}{3} - \hat{G}_M(0) - \hat{G}_M(1)\Big]$$
$$+ \sum_{q=q'}\Big(C_4 + C_6 + \frac{3}{2}e_qC_8 + \frac{3}{2}e_qC_{10}\Big)\Big[\frac{4}{3}\ln\frac{m_b}{\mu} - \hat{G}_M(s_q)\Big] - 2C_{8g}, \tag{2.7b}$$

$$P^{p,ew}_{M,2} = \Big(C_1 + N_cC_2\Big)\Big[\frac{4}{3}\ln\frac{m_b}{\mu} + \frac{2}{3} - G_M(s_p)\Big]$$
$$-\Big(C_3 + N_cC_4\Big)\Big[\frac{4}{3}\ln\frac{m_b}{\mu} + \frac{2}{3} - \frac{1}{2}G_M(0) - \frac{1}{2}G_M(1)\Big]$$
$$+ \sum_{q=q'}\Big(N_cC_3 + C_4 + N_cC_5 + C_6\Big)\frac{3}{2}e_q\Big[\frac{4}{3}\ln\frac{m_b}{\mu} - G_M(s_q)\Big]$$
$$-N_cC_{7\gamma}\int_0^1 dx\ \frac{\Phi_M(x)}{1-x}, \tag{2.7c}$$

$$P^{p,ew}_{M,3} = \Big(C_1 + N_cC_2\Big)\Big[\frac{4}{3}\ln\frac{m_b}{\mu} + \frac{2}{3} - \hat{G}_M(s_p)\Big]$$
$$-\Big(C_3 + N_cC_4\Big)\Big[\frac{4}{3}\ln\frac{m_b}{\mu} + \frac{2}{3} - \frac{1}{2}\hat{G}_M(0) - \frac{1}{2}\hat{G}_M(1)\Big]$$
$$+ \sum_{q=q'}\Big(N_cC_3 + C_4 + N_cC_5 + C_6\Big)\frac{3}{2}e_q\Big[\frac{4}{3}\ln\frac{m_b}{\mu} - \hat{G}_M(s_q)\Big] - N_cC_{7\gamma}. \tag{2.7d}$$

The definitions of quantities $V_M$, $V'_M$, $G_M(s_q)$, and $\hat{G}_M(s_q)$ can be found in [22], and $s_q = m_q^2/m_b^2$. In the expressions for $P^p_{M,i}$ and $P^{p,ew}_{M,i}$, $q'$ will run over all the active quarks at the scale $\mu = \mathcal{O}(m_b)$, i.e., $q' = u, d, s, c, b$. The parameters $H(BM_1, M_2)$ and $H'(BM_1, M_2)$ in $a_{i,II}$, which originate from hard gluon exchanges between the spectator quark and the emitted meson $M_2$, are written as

$$H(BV, P) = \frac{f_Bf_V}{m_B^2A_0^{B\to V}}\int_0^1 d\xi\int_0^1 dx\int_0^1 dy\frac{\Phi_B(\xi)}{\xi}\frac{\Phi_P(x)}{\bar{x}}\frac{\Phi_V(y)}{\bar{y}}, \tag{2.8a}$$

$$H'(BV, P) = \frac{f_Bf_V}{m_B^2A_0^{B\to V}}\int_0^1 d\xi\int_0^1 dx\int_0^1 dy\frac{\Phi_B(\xi)}{\xi}\frac{\Phi_P(x)}{x}\frac{\Phi_V(y)}{\bar{y}}. \tag{2.8b}$$

For case II, except for the parameters of $H(BM_1, M_2)$ and $H'(BM_1, M_2)$, the expressions for $a_i$ are similar to those in case I. In particular, we would like to point out that because

$\langle V|(\bar{q}q)_{S\pm P}|0\rangle = 0$, the contributions of the effective operators $O_{6,8}$ to the hadronic matrix elements vanish, i.e., the terms that are related to $a_{6,8}$ disappear from the decay amplitudes for case II. As to the parameters $H(BM_1, M_2)$ and $H'(BM_1, M_2)$ in $a_{i,II}$, they are defined as

$$H(BP,V) = \frac{f_B f_P}{m_B^2 F_1^{B\to P}} \int_0^1 d\xi \int_0^1 dx \int_0^1 dy \frac{\Phi_B(\xi)}{\xi} \frac{\Phi_V(x)}{\bar{x}} \Big[ \frac{\Phi_P(y)}{\bar{y}} + \frac{2\mu_P}{m} \frac{\bar{x}}{x} \frac{\Phi_P^p(y)}{\bar{y}} \Big], \tag{2.9a}$$

$$H'(BP,V) = -\frac{f_B f_P}{m_B^2 F_1^{B\to P}} \int_0^1 d\xi \int_0^1 dx \int_0^1 dy \frac{\Phi_B(\xi)}{\xi} \frac{\Phi_V(x)}{x} \Big[ \frac{\Phi_P(y)}{\bar{y}} + \frac{2\mu_P}{m} \frac{x}{\bar{x}} \frac{\Phi_P^p(y)}{\bar{y}} \Big]. \tag{2.9b}$$

Now we would like to make some comments on $a_i$

1. It was shown in [27] that at leading order approximation $a_i$ are renormalization scale-independent, i.e.,

$$\frac{d\ a_{i,I}}{d\ \ln\mu} = 0 \quad (i\neq 6,8) \qquad \text{and} \qquad \frac{d\ a_{i,I} r_\chi}{d\ \ln\mu} = 0 \quad (i = 6,8) \tag{2.10}$$

   where $r_\chi$ is the chirally enhanced factor, e.g., $r_\chi^K(\mu) = \frac{2m_{K^+}^2}{m_b(\mu)[m_u(\mu)+m_s(\mu)]}$ for the decay $B^0\to K^+\rho^-$. It is formally $\mathcal{O}(\Lambda_{QCD}/m_b)$ power suppressed, but numerically large. The deviation of the data in Table II from Eq.(2.10) can be reduced further when the higher order radiative corrections to the hadronic matrix elements are included. So in the following calculations, we will fix $\mu = m_b$. In addition, it has been proved that $a_i$ are free of gauge dependence. These two points guarantee that the decay amplitudes are physical.

2. From Eq.(2.6) we can see that, in the heavy quark limit, when the corrections at the order of $\alpha_s$ and $\alpha$ are neglected, we return to the NF approximation.

3. "Nonfactorizable" effects appear at the order of $\alpha_s$ or/and $\Lambda_{QCD}/m_b$. This reflects the fact that the final state interactions are either dominated by hard processes or power suppressed. Therefore the strong phases for the class-I ($a_1$ dominant) decays are small and furthermore perturbatively calculable in the heavy quark limit. Moreover,

from the data in Table II, we find that the "nonfactorizable" effects contribute a large imaginary part to $a_{2,I}$, i.e., the class-II ($a_2$ dominant) decays, especially the CP asymmetries, might be sensitive to the "nonfactorizable" corrections.

### D. The annihilation parameters $b_i$

The parameters of $b_i$ in Eq.(2.5) correspond to weak annihilation contributions. Now we give their expressions, which are analogous to those in [22]:

$$b_1(M_1,M_2)=\frac{C_F}{N_c^2}C_1A_1^i(M_1,M_2),\qquad b_2(M_1,M_2)=\frac{C_F}{N_c^2}C_2A_1^i(M_1,M_2), \tag{2.11a}$$

$$b_3(M_1,M_2)=\frac{C_F}{N_c^2}\Big\{C_3A_1^i(M_1,M_2)+C_5A_3^i(M_1,M_2)+\Big[C_5+N_cC_6\Big]A_3^f(M_1,M_2)\Big\}, \tag{2.11b}$$

$$b_4(M_1,M_2)=\frac{C_F}{N_c^2}\Big\{C_4A_1^i(M_1,M_2)+C_6A_2^i(M_1,M_2)\Big\}, \tag{2.11c}$$

$$b_3^{ew}(M_1,M_2)=\frac{C_F}{N_c^2}\Big\{C_9A_1^i(M_1,M_2)+C_7A_3^i(M_1,M_2)+\Big[C_7+N_cC_8\Big]A_3^f(M_1,M_2)\Big\}, \tag{2.11d}$$

$$b_4^{ew}(M_1,M_2)=\frac{C_F}{N_c^2}\Big\{C_{10}A_1^i(M_1,M_2)+C_8A_2^i(M_1,M_2)\Big\}. \tag{2.11e}$$

Here the current-current annihilation parameters $b_{1,2}(M_1,M_2)$ arise from the hadronic matrix elements of the effective operators $O_{1,2}$, the QCD penguin annihilation parameters $b_{3,4}(M_1,M_2)$ from $O_{3-6}$, and the electroweak penguin annihilation parameters $b_{3,4}^{ew}(M_1,M_2)$ from $O_{7-10}$. The parameters of $b_i$ are closely related to the final states; they can also be divided into two different cases according to the final states. Case I is that $M_1$ is a vector meson, and $M_2$ is a pseudoscalar meson (here $M_1$ and $M_2$ are tagged in Fig.2). Case II is that $M_1$ corresponds to a pseudoscalar meson, and $M_2$ corresponds to a vector meson. For case I, the definitions of $A_k^{i,f}(M_1,M_2)$ in Eq.(2.11) are

$$A_1^f(V,P)=0,\qquad A_2^f(V,P)=0, \tag{2.12a}$$

$$A_3^f(V,P)=\pi\alpha_s\int_0^1dx\int_0^1dy\Phi_V(x)\Phi_P^p(y)\frac{2\mu_P}{m}\frac{2(1+\bar{x})}{\bar{x}^2y}, \tag{2.12b}$$

$$A_1^i(V,P)=\pi\alpha_s\int_0^1dx\int_0^1dy\Phi_V(x)\Phi_P(y)\Big[\frac{1}{y(1-x\bar{y})}+\frac{1}{\bar{x}^2y}\Big], \tag{2.12c}$$

$$A_2^i(V,P)=-\pi\alpha_s\int_0^1dx\int_0^1dy\Phi_V(x)\Phi_P(y)\Big[\frac{1}{\bar{x}(1-x\bar{y})}+\frac{1}{\bar{x}y^2}\Big], \tag{2.12d}$$

$$A_3^i(V,P) = \pi\alpha_s \int_0^1 dx \int_0^1 dy \Phi_V(x)\Phi_P^p(y) \frac{2\mu_p}{m} \frac{2\bar{y}}{\bar{x}y(1-x\bar{y})}. \tag{2.12e}$$

For case-II,

$$A_1^f(P,V) = 0, \qquad A_2^f(P,V) = 0, \tag{2.13a}$$

$$A_3^f(P,V) = -\pi\alpha_s \int_0^1 dx \int_0^1 dy \Phi_P^p(x)\Phi_V(y) \frac{2\mu_P}{m} \frac{2(1+y)}{\bar{x}y^2}, \tag{2.13b}$$

$$A_1^i(P,V) = \pi\alpha_s \int_0^1 dx \int_0^1 dy \Phi_P(x)\Phi_V(y) \Big[\frac{1}{y(1-x\bar{y})} + \frac{1}{\bar{x}^2 y}\Big], \tag{2.13c}$$

$$A_2^i(P,V) = -\pi\alpha_s \int_0^1 dx \int_0^1 dy \Phi_P(x)\Phi_V(y) \Big[\frac{1}{\bar{x}(1-x\bar{y})} + \frac{1}{\bar{x}y^2}\Big], \tag{2.13d}$$

$$A_3^i(P,V) = \pi\alpha_s \int_0^1 dx \int_0^1 dy \Phi_P^p(x)\Phi_V(y) \frac{2\mu_p}{m} \frac{2x}{\bar{x}y(1-x\bar{y})}. \tag{2.13e}$$

Here our notation and convention are the same as those in [22]. The superscripts $i$ and $f$ on $A^{i,f}$ correspond to the contributions from Fig.2(a-b) and Fig.2(c-d), respectively. The subscripts $k = 1, 2, 3$ on $A_k^{i,f}$ refer to the Dirac structures $(V-A)\otimes(V-A)$, $(V-A)\otimes(V+A)$ and $(-2)(S-P)\otimes(S+P)$, respectively. $\Phi_V(x)$ denotes the leading-twist LCDAs of a vector meson, and $\Phi_P(x)$ and $\Phi_P^p(x)$ denote twist-2 and twist-3 LCDAs of a pseudoscalar meson, respectively[1].

Note that assuming $SU(3)$ flavor symmetry and symmetric (under $x \leftrightarrow \bar{x}$) LCDAs of light mesons, we have $A_1^i = -A_2^i$. In this approximation the weak annihilation contributions (for case I) can be parametrized as

---

[1] The expression for $A_3^i$ is different from that in [24]. This difference originates from the two different ways of dealing with the annihilation contribution from the twist-3 LCDAs. Cheng and Yang calculated them in coordinate space, and we take the projection in momentum space given in [22]. We made some investigation of this problem in [27], and discussed it with Beneke et al. The point lies in how to deal with the surface terms in the integral. In addition, we found that, when the annihilation contributions from the twist-3 LCDAs are considered for $B \to PP$ decays in coordinate space, not only logarithmic divergence but also linear and quadratic divergences appear, which is a very serious problem. So we use the method given in [22], which gives only a logarithmic divergence even for $B \to PP$ decays.

$$A_1^i(V,P)\simeq 18\pi\alpha_s\Big(X_A-4+\frac{\pi^2}{3}\Big), \tag{2.14a}$$

$$A_3^i(V,P)\simeq \pi\alpha_s r_\chi\Big[2\pi^2-6\Big(X_A^2+2X_A\Big)\Big], \tag{2.14b}$$

$$A_3^f(V,P)\simeq 6\pi\alpha_s r_\chi\Big(2X_A^2-X_A\Big), \tag{2.14c}$$

where $X_A = \int_0^1 dx/x$ parametrizes the divergent endpoint integrals. We can get similar forms to Eq.(2.14) for case II, but with $A_3^f(P,V) = -A_3^f(V,P)$. In our calculation, we will treat $X_A$ as a phenomenological parameter, and take the same value for all annihilation terms, although this approximation is crude and there is no known physical argument for justifying this assumption. We shall see below that $X_A$ gives large uncertainties in the theoretical prediction.

## III. INPUT PARAMETERS

The QCDF expressions for the hadronic matrix elements are written as the product of hard-scattering kernels and LCDAs of mesons. The hard scattering kernels are perturbatively calculable, while the soft and nonperturbative effects are incorporated into two kinds of universal parameter: the form factors and the LCDAs of mesons. The decay amplitudes are also related to the CKM matrix elements, the masses of quarks and mesons, various decay constants of mesons, and so on. We will specify them in the following discussions.

### A. The CKM matrix elements

The CKM matrix is described by four independent parameters. Using the Wolfenstein parametrization [33], it can be expressed as

$$V_{CKM} = \begin{pmatrix} 1-\lambda^2/2 & \lambda & A\lambda^3(\rho-i\eta) \\ -\lambda & 1-\lambda^2/2 & A\lambda^2 \\ A\lambda^3(1-\rho-i\eta) & -A\lambda^2 & 1 \end{pmatrix} + \mathcal{O}(\lambda^4). \tag{3.1}$$

Two of them are well-determined: $A = 0.819\pm0.040$ and $\lambda = 0.2237\pm0.0033$ [36]. Recently M. Ciuchini revised the values of $\rho$ and $\eta$ in [37] $\bar{\rho} = 0.218\pm0.038$, $\bar{\eta} = 0.316\pm0.040$, and

$\gamma = (55.5\pm6.2)^\circ$. This gives $\rho = 0.224\pm0.039$ and $\eta = 0.324\pm0.039$. A. Höcker, et al. [38] advocate another approach to a global CKM matrix analysis, using the frequentist statistics named *R*fit; their best fit results are $A = 0.83\pm0.07$, $\lambda = 0.222\pm0.004$, $\bar{\rho} = 0.21\pm0.12$, $\bar{\eta} = 0.38\pm0.11$ and $\gamma = (62\pm15)^\circ$ at 95% confidence level. H. Lacker and M. Neubert et al. suggest that it is possible to derive constraints on $\gamma$ from a global *R*fit analysis of various CP-averaged branching ratios $B\to\pi\pi, \pi K$; their best fit of the QCDF theory to the data yields $(\bar{\rho}, \bar{\eta}) = (0.05, 0.381)$ with $\chi^2/n_{dof} = 0.46$ [39], and correspondingly $\gamma\simeq83^\circ$. In our calculation, we will take the central values of the results in [37] as input parameters. At the same time, we will also give estimations based on the results in [39].

### B. Quark masses

The masses of quarks appear in our calculations in two different ways. The pole masses of quarks arise from the loop integration over the virtual internal quarks in penguin correction diagrams. They contribute to the penguin parameters $P^p_{M,i}$ and $P^{p,ew}_{M,i}$ in Eq.(2.7) in terms of $G_M(s_q)$ and $\hat{G}_M(s_q)$ [22], where $s_q = m_q^2/m_b^2$. We fix them as

$$m_u = m_d = m_s = 0, \quad m_c = 1.45\text{GeV}, \quad m_b = 4.6\text{GeV}. \tag{3.2}$$

The other type of quark mass is the running quark mass which is renormalization scale-dependent. It appears in terms of the chirally enhanced factor $r_\chi$ which arises from the hadronic matrix elements of $(S+P)\otimes(S-P)$ operators through the equations of motion, and the twist-3 LCDAs of the pseudoscalar mesons. Estimations of the running quark masses within the QCD sum rules approach are collected in [40]. Here we would like to use the central values of Particle Data Group 2000 data [41] for discussion.

$$\overline{m}_b(\overline{m}_b) = 4.2\text{GeV}, \qquad \overline{m}_s(2\text{GeV}) = 122.5\text{MeV}, \tag{3.3a}$$

$$\overline{m}_d(2\text{GeV}) = 6\text{MeV}, \qquad \overline{m}_u(2\text{GeV}) = 3\text{MeV}. \tag{3.3b}$$

Using the renormalization group equation, we can get their corresponding values at the scale $\mu = \mathcal{O}(m_b)$. In addition, we would like to point out that, because the running masses

of light quarks have large uncertainties, we will take the $r_\chi^{\eta^{(\prime)}}(1-f_{\eta^{(\prime)}}^u/f_{\eta^{(\prime)}}^s)\simeq r_\chi^\pi\simeq r_\chi^K\equiv r_\chi$ approximation for simplicity in our numerical calculations.

### C. The form factors and decay constants

Now let us parametrize the hadronic matrix elements of $\langle PV|O_i|B\rangle_f$ in Eq.(2.4). After Fierz reordering, with the NF assumption [18], they can be written as

$$\langle PV|O_i|B\rangle = Z_1\langle P|J^\mu|0\rangle\langle V|J_\mu|B\rangle + Z_2\langle V|J'^\mu|0\rangle\langle P|J'_\mu|B\rangle, \tag{3.4}$$

where $J^\mu$ and $J'^\mu$ are hadronic currents and $Z_{1,2}$ are the corresponding coefficients. The hadronic current matrix elements are defined as follows [18]:

$$\langle P(l)|\bar q\gamma^\mu\gamma_5 q|0\rangle = -if_P l^\mu, \qquad \langle V(l,\epsilon)|\bar q\gamma^\mu q|0\rangle = f_V m_V\epsilon^{*\nu}, \tag{3.5a}$$

$$\langle P(l)|\bar q\gamma^\mu(1-\gamma_5)q|B\rangle = \Big[p_B^\mu + l^\mu - \frac{m_B^2-m_P^2}{k^2}k^\mu\Big]F_1(k^2) + \frac{m_B^2-m_P^2}{k^2}k^\mu F_0(k^2), \tag{3.5b}$$

$$\begin{aligned}\langle V(l,\epsilon)|\bar q\gamma_\mu(1-\gamma_5)q|B\rangle &= \epsilon_{\mu\nu\alpha\beta}\epsilon^{*\nu}p_B^\alpha l^\beta\frac{2V(k^2)}{m_B+m_V} + i\frac{2m_V(\epsilon^*\cdot k)}{k^2}k_\mu A_0(k^2)\\ &+ i\epsilon_\mu^*(m_b+m_V)A_1(k^2) - i\frac{\epsilon^*\cdot k}{m_b+m_V}(p_B+l)_\mu A_2(k^2)\\ &- i\frac{2m_V(\epsilon^*\cdot k)}{k^2}k_\mu A_3(k^2),\end{aligned} \tag{3.5c}$$

where $k=p_B-l$, and $\epsilon^*$ denotes the polarization vector of the vector meson $V$. $f_P$ and $f_V$ are decay constants, and $F_{0,1}(k^2)$, $V(k^2)$, and $A_{0,1,2,3}(k^2)$ are form factors. In addition, at the poles $k^2=0$, we have

$$F_0(0)=F_1(0), \qquad A_0(0)=A_3(0), \tag{3.6a}$$

$$2m_V A_3(0) = (m_B+m_V)A_1(0) - (m_B-m_V)A_2(0). \tag{3.6b}$$

In the QCDF framework, they are all nonperturbative quantities, and appear as universal input parameters. As a good approximation, we take these form factors at $k^2=0$ in our calculations.

Because the flavor octet mixes with the flavor singlet in the $SU(3)$ quark representation of mesons, the corresponding hadronic parameters are difficult to determine. Here we assume

ideal mixing between $\omega$ and $\phi$, i.e., $\omega = (u\bar{u}+d\bar{d})/\sqrt{2}$ and $\phi = s\bar{s}$. As to $\eta$ and $\eta'$, we follow the convention in [29,42,43]: the two-mixing-angle formula is applied for the decay constants and form factors, and the charm quark content in $\eta$ and $\eta'$ is assumed to be negligible:

$$\langle 0|\bar{q}\gamma_\mu\gamma_5 q|\eta^{(\prime)}(p)\rangle = if^q_{\eta^{(\prime)}}p_\mu, \qquad (q=u,d,s) \tag{3.7a}$$

$$\frac{\langle 0|\bar{u}\gamma_5 u|\eta^{(\prime)}\rangle}{\langle 0|\bar{s}\gamma_5 s|\eta^{(\prime)}\rangle} = \frac{f^u_{\eta^{(\prime)}}}{f^s_{\eta^{(\prime)}}}, \qquad \langle 0|\bar{s}\gamma_5 s|\eta^{(\prime)}\rangle = -i\frac{m^2_{\eta^{(\prime)}}}{2m_s}(f^s_{\eta^{(\prime)}} - f^u_{\eta^{(\prime)}}), \tag{3.7b}$$

$$f^u_\eta = \frac{f_8}{\sqrt{6}}\cos\theta_8 - \frac{f_0}{\sqrt{3}}\sin\theta_0, \qquad f^s_\eta = -2\frac{f_8}{\sqrt{6}}\cos\theta_8 - \frac{f_0}{\sqrt{3}}\sin\theta_0, \tag{3.7c}$$

$$f^u_{\eta'} = \frac{f_8}{\sqrt{6}}\sin\theta_8 + \frac{f_0}{\sqrt{3}}\cos\theta_0, \qquad f^s_{\eta'} = -2\frac{f_8}{\sqrt{6}}\sin\theta_8 + \frac{f_0}{\sqrt{3}}\cos\theta_0, \tag{3.7d}$$

$$F^{B\eta}_{0,1} = F^{B\pi}_{0,1}\Big(\frac{\cos\theta_8}{\sqrt{6}} - \frac{\sin\theta_0}{\sqrt{3}}\Big), \qquad F^{B\eta'}_{0,1} = F^{B\pi}_{0,1}\Big(\frac{\sin\theta_8}{\sqrt{6}} + \frac{\cos\theta_0}{\sqrt{3}}\Big). \tag{3.7e}$$

We take the mixing angles as $\theta_8 = -22.2^\circ$ and $\theta_0 = -9.1^\circ$. For the $B\to K$ transition form factors we use the $SU(3)$ flavor symmetry approximation

$$\frac{f_\pi}{f_K}\approx\frac{F^{B\pi}_{0,1}(0)}{F^{BK}_{0,1}(0)}. \tag{3.8}$$

The decay constants and form factors are nonperturbative parameters; they are available from the experimental data and/or estimated with well-founded theories, such as lattice calculations, QCD sum rules etc. Now we take their values in our calculations as [29,41,44–47]:

$$f_\pi = 131\text{MeV}, \qquad f_K = 160\text{MeV}, \qquad f_{K^*} = 214\text{MeV},$$
$$f_\rho = 210\text{MeV}, \qquad f_\omega = 195\text{MeV}, \qquad f_\phi = 233\text{MeV},$$
$$f_0 = 157\text{MeV}, \qquad f_8 = 168\text{MeV}, \qquad f_B = 180\text{MeV},$$
$$F^{B\pi}_{0,1}(0) = 0.28\pm0.05, \qquad A^{BK^*}_0(0) = 0.39\pm0.10,$$
$$A^{B\rho}_0(0) = 0.30\pm0.05, \qquad A^{B\omega}_0(0) = 0.30\pm0.05.$$

### D. The LCDAs of mesons

The LCDAs of mesons are also basic input parameters in the QCDF formula Eq.(2.3). The LCDAs of light pseudoscalar mesons are defined as [48]:

$$\langle P(k)|\bar{q}(z_2)q(z_1)|0\rangle$$
$$= \frac{if_P}{4}\int_0^1 dx\ e^{i(xk\cdot z_2+\bar{x}k\cdot z_1)}\Big\{\not{k}\gamma_5\Phi_P(x) - \mu_P\gamma_5\Big[\Phi_P^p(x) - \sigma_{\mu\nu}k^\mu z^\nu\frac{\Phi_P^\sigma(x)}{6}\Big]\Big\}, \tag{3.9}$$

where $f_P$ is a decay constant. $z = z_2 - z_1$, $\bar{x} = 1 - x$, and $\mu_P = \frac{m_P^2}{[m_1(\mu)+m_2(\mu)]}$ (here $m_1$ and $m_2$ are running masses of the valence quarks of the pseudoscalar meson ($P$) with mass $m_P$.), $\Phi_P(x)$ is the leading twist LCDAs, and $\Phi_P^p(x)$, $\Phi_P^\sigma(x)$ are twist-3 LCDAs of the meson. We shall use the asymptotic forms of the LCDAs for the following discussion:

$$\Phi_P(x) = 6x\bar{x}, \qquad \Phi_P^p(x) = 1, \qquad \Phi_P^\sigma(x) = 6x\bar{x}. \tag{3.10}$$

The twist-2 LCDAs of the vector mesons are defined as [47,49]:

$$\langle 0|\bar{q}(0)\sigma_{\mu\nu}q(z)|V(k,\lambda)\rangle = i(\epsilon_\mu^\lambda k_\nu - \epsilon_\nu^\lambda k_\mu)f_V^\perp\int_0^1 dx\ e^{-ixk\cdot z}\Phi_V^\perp(x), \tag{3.11a}$$

$$\langle 0|\bar{q}(0)\gamma_\mu q(z)|V(k,\lambda)\rangle = k_\mu\frac{\epsilon^\lambda\cdot z}{k\cdot z}f_V m_V\int_0^1 dx\ e^{-ixk\cdot z}\Phi_V^\parallel(x), \tag{3.11b}$$

where $\epsilon$ is a polarization vector, and for longitudinally polarized mesons $\epsilon_\parallel = k/m_V$. $\Phi_V^\parallel(x)$ and $\Phi_V^\perp(x)$ describe the quark distributions of transversely and longitudinally polarized mesons. In our calculations, the contributions from $\Phi_V^\perp(x)$ are power suppressed and hence can be neglected, i.e., we take the following approximation:

$$\Phi_V(x) = \Phi_V^\parallel(x) = 6x\bar{x}. \tag{3.12}$$

For the wave function of the B meson, we take the form in [34,35,50]:

$$\Phi_B(\xi) = N_B\xi^2(1-\xi)^2\exp\Big[-\frac{m_B^2\xi^2}{2\omega_B^2}\Big], \tag{3.13}$$

where $N_B$ is the normalization constant. $\Phi_B(\xi)$ is peaked around $\xi\approx 0.1$ with $\omega_B = 0.4$GeV.

With these LCDAs of the mesons, we still cannot get the parameters $a_i$ and $b_i$ at once, because we will encounter endpoint divergence in dealing with the integrals Eq.(2.9), Eq.(2.12), and Eq.(2.13). If the transverse momentum $k_\perp$ of the partons and the Sudakov resummation can be taken into account consistently in the QCDF approach, the above-mentioned integrals might be convergent. But now we have to treat these divergent integrals as phenomenological parameters:

$$X = \int_0^1 \frac{dx}{x} = \ln\frac{m_B}{\overline{\Lambda}} + \varrho e^{-i\phi}, \tag{3.14}$$

where $\varrho$ can vary from 0 to 6, $\phi$ is an arbitrary phase, and $0°\leq\phi\leq360°$. These notations are almost the same as those in [22,24]. In our calculation, $X_H$ and $X_A$ denote the endpoint divergent integrals from hard spectator scattering Eq.(2.9), and weak annihilations Eq.(2.12), Eq.(2.13), respectively. We take $\overline{\Lambda} = \Lambda_{QCD}$ and $\varrho e^{-i\phi} = i\pi$ as default values.

## IV. BRANCHING RATIOS

The branching ratios of charmless decays $B\to PV$ in the B meson rest frame can be written as

$$\mathcal{B}r(B\to PV) = \frac{\tau_B}{8\pi}\frac{|p|}{m_B^2}|\mathcal{A}(B\to PV)|^2. \tag{4.1}$$

In our calculation, we take $\tau_{B^0} = 1.548$ps, $\tau_{B^\pm} = 1.653$ps, and

$$|p| = \frac{\sqrt{[m_B^2-(m_P+m_V)^2][m_B^2-(m_P-m_V)^2]}}{2m_B}. \tag{4.2}$$

Since QCD factorization works in the heavy quark limit, the above masses of light mesons should be taken as zero for consistency.

The experimental measurements are collected in Table III. Our numerical results for CP-averaged branching ratios for $B\to PV$ are listed in Table IV and Table V, calculated at the scale $\mu = m_b$ for two choices of CKM matrix elements: (1) $A = 0.819$, $\lambda = 0.2237$, $\bar{\rho} = 0.218$, and $\bar{\eta} = 0.316$ [37]; (2) $A = 0.83$, $\lambda = 0.222$, $\bar{\rho} = 0.05$, and $\bar{\eta} = 0.381$ [39]. The other related parameters are taken at their default values. In the tables, $\mathcal{B}r$ stands for the values that are calculated without including weak annihilation contributions within the NF framework; $\mathcal{B}r^f\propto|\mathcal{A}^f|^2$ and $\mathcal{B}r^{f+a}\propto|\mathcal{A}^f+\mathcal{A}^a|^2$ are estimated with the QCDF approach where $\mathcal{A}^a$ denotes the annihilation contributions. Since the above two choices of CKM matrix elements are nearly equivalent to two choices of the angle $\gamma$, many of the CP-averaged branching ratios are similar to each other for these two sets of CKM matrix elements, as can be seen from Table IV and Table V. Only the decay channels that have large interference between tree

and penguin contributions are sensitive to the angle $\gamma$, such as $\overline{B}^0 \to \pi^+ K^{*-}$ and $B^- \to \pi^0 K^{*-}$. It is thus possible to extract $\gamma$ from these decay channels. However, we must consider the uncertainties due to the variations of various parameters, such as form factors, and the model dependence of the parametrization of chirally enhanced hard-spectator contributions and annihilation contributions, and so on. Nevertheless, it is still possible to obtain some information on $\gamma$ with detailed analysis. The readers may notice that some numerical results in Table IV and Table V are inconsistent with the experimental measurements listed in Table III. The inconsistency is not serious because we use default values of the parameters for the tables and do not consider the uncertainties from the input parameters. In fact, we will see that for appropriate regions of parameters predictions from the QCDF approach are in agreement with current measurements for most of the $B \to PV$ decays.

From the experience in $B \to PP$ analysis [28], we know that the main theoretical uncertainties of branching ratios come from CKM matrix elements, form factors, and weak annihilation contributions. It is easy to imagine the importance of CKM matrix elements and form factors, but for weak annihilation topologies the importance was first noticed recently in [34] within the perturbative QCD approach. However, within the QCDF framework, the annihilation topologies introduce endpoint divergence, which violates factorization; in Ref. [22], the authors phenomenologically parametrize the endpoint divergence integral as $X_A$. In this work, we will follow their way of estimating the annihilation contributions, although it will introduce model dependence and numerical uncertainties.

We know that the leading power of the annihilation contribution is always $X_A^2$ for $B \to PP$ decay amplitudes. But for $B \to PV$, the case is different: According to the formulas in Sec. II D, $b_3^{ew}$ and $b_4^{ew}$ are negligible in general because of small Wilson coefficients, and $b_4$ is also small due to the cancellation between $A_1^i$ and $A_2^i$. For the other $b_i$ parameters we have

$$b_1 = \frac{C_F}{N_c^2} C_1 A_1^i = 18 \frac{C_F}{N_c^2} C_1 \pi \alpha_s (X_A + \frac{\pi^2}{3} - 4), \tag{4.3}$$

$$b_2 = \frac{C_F}{N_c^2} C_2 A_1^i = 18 \frac{C_F}{N_c^2} C_2 \pi \alpha_s (X_A + \frac{\pi^2}{3} - 4), \tag{4.4}$$

$$b_3 \simeq \frac{C_F}{N_c^2} N_c C_6 A_3^f = \pm 6 \frac{C_F}{N_c^2} N_c C_6 r_\chi \pi \alpha_s (2X_A^2 - X_A). \tag{4.5}$$

So when $b_1$ or $b_2$ dominates the leading power of the annihilation contributions is $X_A$. This indicates that in some cases, compared with $B \to PP$ decays (where $X_A^2$ appears), annihilation topologies might introduce smaller uncertainties into $B \to PV$ branching ratios.

In the following we will proceed to analyze some decay modes for $B \to PV$ in detail.

### A. $B^0 \to \pi^\pm \rho^\mp$ decays

From Table III and Table IV, we can see that the theoretical estimation of the CP-averaged branching ratio $\mathcal{B}r(B^0 \to \pi^+\rho^- + \pi^-\rho^+)$ is in agreement with the measurements of the BaBar and CLEO Collaborations within one standard deviation, especially when we consider the uncertainties due to the variations of input parameters (see Fig.3).

The decays of $B^0 \to \pi^\pm \rho^\mp$ are $a_1$ dominant. The "nonfactorizable" contributions are small, so there is no distinct difference between the results obtained with the QCDF approach and those with the NF approach. We can see this point from Table IV. The annihilation amplitudes of these decay channels are $b_1$ dominant, so they do not contribute large uncertainties to the branching ratios. From Fig. 3(c), it is obvious that the hard spectator scattering has little impact on the branching ratio. Therefore the main uncertainties in the CP-averaged branching ratios of these decay modes originate from the form factors and CKM matrix elements (especially $|V_{ub}|$), as can be seen from Fig.3.

The ratio of branching ratios $\frac{\mathcal{B}r(B^0 \to \pi^-\rho^+)}{\mathcal{B}r(B^0 \to \pi^+\rho^-)}$ has been discussed in [29]. From Fig.3(f), it is obvious that $\mathcal{B}r(B^0 \to \pi^-\rho^+) > \mathcal{B}r(B^0 \to \pi^+\rho^-)$, mainly due to the difference between the decay constants: $f_\rho > f_\pi$. In addition, the destructive interference among penguin amplitudes also lowers the branching ratio of $B^0 \to \pi^+\rho^-$, although this effect is relatively small. In fact, because the decay constants of vector mesons are generally larger than those of pseudoscalar mesons, i.e., $f_V > f_P$, it seems universal that, for the $a_1$ dominant $B \to PV$ decay modes, the decay channels with emitted vector mesons have larger branching ratios than the corresponding decay channels with emitted pseudoscalar mesons. From Fig.3(a),

it is clear that the averaged branching ratio of these decays is only mildly dependent on the angle $\gamma$, which hints the small contribution from penguin amplitudes. So it is reasonable to neglect the penguin amplitudes, which leads to

$$\frac{\mathcal{B}r(B^0\to\pi^-\rho^+)}{\mathcal{B}r(B^0\to\pi^+\rho^-)}\approx\Big[\frac{f_\rho F_1^{B\pi}(0)}{f_\pi A_0^{B\rho}(0)}\Big]^2. \tag{4.6}$$

Clearly, this ratio is insensitive to the CKM matrix elements, dynamical coefficients $a_i$, and so on. Since it relates different form factors, a measurement of this ratio may be helpful to improve theoretical predictability. We draw this ratio versus $\gamma$ in Fig.3(f).

### B. $B^-\to\pi\rho,\pi\omega$ decays

The decays $B^-\to\pi\rho,\pi\omega$ are also tree dominant, but they are determined by $a_1+\xi a_2$. From Fig.4(a) and Fig.5(a), we can see that within appropriate ranges of the parameters, our results for $\mathcal{B}r(B^-\to\pi^-\rho^0)$ and $\mathcal{B}r(B^-\to\pi^-\omega)$ are in good agreement with the measurements. For $\mathcal{B}r(B^-\to\pi^0\rho^-)$, the branching ratio is predicted numerically to be large and it should be observed readily, although there is only an experimental upper limit so far.

Generally speaking, for the branching ratios, the numerical uncertainties due to the variations of the CKM matrix elements and form factors are always large. But it is distinctive for $B^-\to\pi\rho,\pi\omega$ decays that hard spectator scattering also causes sizable uncertainties [about 20%; see Fig. 4(c) and Fig. 5(c)]. This is because, as mentioned above, these decay modes are determined by $a_1+\xi a_2$ and "nonfactorizable" effects; in particular, terms of hard spectator scattering contribute greatly to $a_2$. As for annihilation contributions, due to the cancellations such as $b_2(P,V)-b_2(V,P)$ and $b_3(P,V)+b_3(V,P)$, $A^a(B^-\to\pi^-\rho^0)$ and $A^a(B^-\to\pi^-\omega)$ are dominated by $b_3$ and $b_2$, respectively. So for $B^-\to\pi^-\rho^0$ the annihilation topologies also contribute large uncertainties to the branching ratio, while for $B^-\to\pi^-\omega$, the uncertainty due to the annihilation parameter $X_A$ is negligible [see Fig 4(b) and Fig 5(b)].

### C. $B \to K\phi$ decays

The decays $B^0 \to K^0\phi$ and $B^- \to K^-\phi$ have triggered great theoretical interest [24,29,30,51] because they are pure penguin processes. Experimentally, these two decay modes have been observed by the BaBar, Belle and CLEO Collaborations; the averaged measurements ignoring correlations are $\mathcal{B}r(B^0 \to K^0\phi) = (7.5 \pm 1.8) \times 10^{-6}$ and $\mathcal{B}r(B^- \to K^-\phi) = (7.9 \pm 1.2) \times 10^{-6}$. Our results within the QCDF framework are in good agreement with the experimental data within $1\sigma$ [see Fig.6(a,b)].

From the expressions for the decay amplitudes in Appendix B of [29], we can see that the decays $B \to K\phi$ only relate to the CKM factor $V_{tb}V_{ts}^*$, which is well determined experimentally. So the decay rates are independent of the angle $\gamma$ and the uncertainties due to the variations of the CKM parameters should be very small.

For $B \to K\phi$ decays, it is very interesting that the prediction is much different between the generalized factorization (GF) approach and the QCDF approach. Within the GF framework, the predicted branching ratios of the decays $B \to K\phi$ are very sensitive to the "nonfactorizable" effects, they vary from $18 \times 10^{-6}$ to $0.4 \times 10^{-6}$ [29] (or from $13 \times 10^{-6}$ to $0.3 \times 10^{-6}$ [20]) with the effective number of colors $N_c^{eff} = 2 \sim \infty$. But within the QCDF framework, there is no need to introduce the effective color number $N_c^{eff}$. However, since $A^a(B \to K\phi)$ is dominated by $b_3$, the branching ratios will be very sensitive to the annihilation parameter $X_A$. As for hard spectator scattering, since $\mathcal{A}^f(B \to K\phi)$ is dominated by $a_4$, the uncertainties from the variations of $X_H$ should be small. In [24], the authors also analyzed the decays $B \to K\phi$ with the QCDF approach. The effects of the twist-3 LCDAs of $K$ mesons on the hard spectator interactions were considered there in spite of their small corrections to the decay amplitudes. When the contributions from the weak annihilations are taken into account, their predictions are $\mathcal{B}r(B^0 \to K^0\phi) = (4.0^{+2.9}_{-1.4}) \times 10^{-6}$ and $\mathcal{B}r(B^- \to K^-\phi) = (4.3^{+3.0}_{-1.4}) \times 10^{-6}$ (their central values correspond to $\varrho_H = \varrho_A = 0$), which are consistent with our estimation at $\mu = m_b$, although the values of input parameters are slightly different.

### D. $B \to \eta K^*$ decays

The $B \to \eta K^*$ decays are well established experimentally by the BaBar, Belle, and CLEO Collaborations (see Table III). But within the QCDF framework our estimations (see Table V) using default input parameters are several times smaller than the experimental measurements. Even considering the large numerical uncertainties, the predicted branching ratios are only marginally consistent with the experiments [see Fig. 6(c,d)].

In fact, there is a similar problem for $B \to \eta^{(\prime)} K$ decays which aroused intense discussion several years ago (see, for example, Refs. [52–57]). It is now commonly believed that this puzzle may be related to a special property of $\eta'$: it has large coupling with two gluons [55,56]. However, there are definitely no large $\eta gg$ contributions to the decay amplitudes of $B \to \eta K^*$.

Here we would like to point out that the CP-averaged branching ratios for $B \to \eta' K^*$ decays are similar to those for $B \to \eta K^*$ decays with the default parameters (see Table V), which are different from the results listed in [20,29,57]. H. Cheng and K. Yang thought that $\mathcal{B}r(B \to \eta K^*)$ should be much larger than $\mathcal{B}r(B \to \eta' K^*)$ in the GF approach, and their favorable values are $\frac{\mathcal{B}r(B^0 \to \eta K^{*0})}{\mathcal{B}r(B^0 \to \eta' K^{*0})} \simeq 20$ and $\frac{\mathcal{B}(B^- \to \eta K^{*-})}{\mathcal{B}r(B^- \to \eta' K^{*-})} \simeq 18$ with $N_c^{eff}(LL) = 2$ and $N_c^{eff}(LR) = 6$ [20]. In [29], A. Ali *et al.* predicted that $\mathcal{B}r(B \to \eta' K^*)$ would be too small to exceed $1 \times 10^{-6}$. In those works [20,29,57], the small branching ratios for $B \to \eta' K^*$ decays are due to delicate cancellation between different parts of the decay amplitudes. However, this cancellationis sensitive to the choice of the input parameters such asform factors and so on (see Table. IV in [20]). In our analyses, we find that the weak annihilation contributions might cause large uncertainties in the predictions of $B \to \eta^{(\prime)} K^*$ decays.

Let us have a closer look at the numerical uncertainties of $\mathcal{B}r(B \to \eta K^*)$. Their decay amplitudes are penguin dominant, so for the CKM factors only $|V_{tb} V_{ts}^*|$ plays an important role. Since $|V_{tb} V_{ts}^*|$ is well determined experimentally, we do not expect large uncertainties from the CKM parameters. As for hard spectator scattering, since $a_4$ and $a_6$ are the most important coefficients in the amplitudes, the hard spectator parameter $X_H$ has a small effect

on the branching ratios. The decay amplitudes also depend on the form factors $F_1^{B\to\eta}$ and $A_0^{B\to K^*}$, but it seems unlikely that the form factors would be dramatically different from the default values. Fortunately, the annihilation contribution is dominated by $b_3$, which could bring large uncertainties to the branching ratios. However, considering the big gap between experiments and default numerical predictions, the annihilation parameter $X_A$ should be very large. In this paper, we choose the model that $X_A$ is universal for all $B\to PV$ channels, and even universal for all $B\to PP$ channels [28], so is it possible for a large $X_A$ to survive for a global $B\to PV$ and $PP$ fit? It may be a challenge for the QCDF approach to obtain a large $\mathcal{B}r(B\to\eta K^*)$.

### E. Other decay modes

There are still some decay modes for $B\to PV$ where the QCDF predictions are marginally consistent or even inconsistent with the experimental results, such as $B^-\to\pi^-\overline{K}^{*0}$ and $\overline{B}^0\to K^-\rho^+, \pi^+K^{*-}$ (see Fig. 6). As an illustration, let us see what the QCDF prediction for $B^-\to\pi^-\overline{K}^{*0}$ and its uncertainties are. Without considering annihilation topologies, this decay channel is a pure penguin process and dominated by the QCD coefficient $a_4$ and the CKM factor $|V_{tb}V_{ts}^*|$. So the branching ratio is independent of the angle $\gamma$, and the variation of the CKM parameters and hard spectator parameter will have very little effect on the decay rate. As for the form factors, only $F^{B\to\pi}$ is involved. But from the experience of $B\to\pi\pi$ [28] we know that it is favorable to have a small form factor. Hence we need a large annihilation parameter $X_A$ again. This indicates that soft interactions play a very important role in some cases. Anyway, it is not good news because the soft annihilation part is model dependent. As we know, annihilation topologies are very important for $B\to PP$ decays; therefore it is very important to check whether a large $X_A$ could be acceptable for other decay modes, such as $B\to\pi\pi$ and $\pi K$. Experimentally, it is also important to search for pure annihilation processes, such as $B^0\to K^+K^-$ and $K^\pm K^{*\mp}$, which may be helpful in learning more about the annihilation mechanism.

Within the QCDF framework, some $B\to PV$ decay modes are predicted to have small branching ratios. One type is the $a_2$ dominant neutral B decays, such as $\overline{B}^0\to\pi^0\rho^0, \pi^0\omega, \eta^{(\prime)}\rho^0, \eta^{(\prime)}\omega$ etc. Another type is those decays whose tree amplitudes are denoted by $a_2$ and suppressed by the CKM factors; moreover, the interference among penguin amplitudes is destructive, for example, the decays $\overline{B}^0\to\overline{K}^0\rho^0, \overline{K}^0\omega$ can be classified into this type. The third type is pure penguin processes including $B^-\to\overline{K}^0\rho^-, K^0K^{*-}$ and $\overline{B}^0\to K^0\overline{K}^{*0}$; their small branching ratios are due to the delicate cancellations among various competing terms. The last type is those decays that are governed by the small coefficients $a_i$, or electroweak penguin dominant decays, including $B^-\to\phi\pi^-$ and $\overline{B}^0\to\phi\pi^0, \phi\eta^{(\prime)}$, etc. Our numerical results in Table IV and Table V indicate that the CP-averaged branching ratios of the above-mentioned decay modes are indeed small, and do not exceed $1\times10^{-6}$ without considering the uncertainties. They are much below the corresponding experimental upper limits. But for these decays, the effects of weak annihilations, soft final-state interactions, and other kinds of power corrections might be very important or even dominant.

## V. CP VIOLATION

CP violation and quark mixing are closely related to each other in the SM. The existence of a CP-violating phase in the top sector of the CKM matrix has been established, i.e., $\mathrm{Im}(V_{td})\propto\bar{\eta}\neq0$. Large CP-violating effects are anticipated and have been observed in the B meson system. In this section, we will study CP violation for charmless decays of $B\to PV$ within the QCDF approach.

Suppose that the decay amplitude for $B\to f$ can be expressed as

$$\mathcal{A}(B\to f) = A_1 e^{-i\xi_1} e^{-i\delta_1} + A_2 e^{-i\xi_2} e^{-i\delta_2}, \tag{5.1}$$

where the $A_i$ are the magnitudes, and $\xi_i$ and $\delta_i$ are the strong and weak phases, respectively. Then we can get the CP-violating asymmetries

$$\mathcal{A}_{CP} = \frac{\Gamma(B\to f) - \Gamma(\overline{B}\to\bar{f})}{\Gamma(B\to f) + \Gamma(\overline{B}\to\bar{f})} = \frac{|\mathcal{A}(B\to f)|^2 - |\mathcal{A}(\overline{B}\to\bar{f})|^2}{|\mathcal{A}(B\to f)|^2 + |\mathcal{A}(\overline{B}\to\bar{f})|^2}$$

$$= \frac{2A_1A_2\sin(\xi_1-\xi_2)\sin(\delta_1-\delta_2)}{A_1^2+A_2^2+2A_1A_2\cos(\xi_1-\xi_2)\cos(\delta_1-\delta_2)}, \tag{5.2}$$

clearly, $\mathcal{A}_{CP}\propto\sin(\xi_1-\xi_2)$. So we would like to repeat some remarks. (1) Within the NF framework, there are no direct CP violations for the hadronic charmless two-body B decays, because in the decay amplitudes the Wilson coefficients and the hadronic matrix elements which are expressed by the product of the decay constants and form factors, are all real, so the strong phase shift $\xi_1-\xi_2=0$. This indicates that "nonfactorizable" effects are important for CP violations in hadronic B decays. (2) In the QCDF framework, the CP violations for the class I ($a_1$ dominant) decay modes should be small, because the strong phases arise at the order of $\alpha_s$ and/or $\Lambda_{QCD}/m_b$, and hence $\sin(\xi_1-\xi_2)$ is small in general. For class II ($a_2$ dominant) decay modes, since $a_{2,I}$ has a large imaginary part (see Table II), a large CP violation might occur.

For charged B decays, the final states are self-tagging. The direct CP-violating asymmetries are defined as

$$\mathcal{A}_{CP} = \frac{\Gamma(B^-\to f^-)-\Gamma(B^+\to f^+)}{\Gamma(B^-\to f^-)-\Gamma(B^+\to f^+)}. \tag{5.3}$$

For neutral B mesons, effects of $B^0$-$\overline{B}^0$ oscillation will induce CP asymmetries, so time-dependent measurements of CP-violating asymmetries are needed:

$$\mathcal{A}_{CP}(t) = \frac{\Gamma(\overline{B}^0(t)\to\bar{f})-\Gamma(B^0(t)\to f)}{\Gamma(\overline{B}^0(t)\to\bar{f})+\Gamma(B^0(t)\to f)}. \tag{5.4}$$

As discussed in [29,58], here we consider three cases for decays of $\overline{B}^0$ and $B^0\to PV$.

- case 1: $B^0\to f$, $\overline{B}^0\to\bar{f}$, but $B^0\not\to\bar{f}$, $\overline{B}^0\not\to f$, for example, $\overline{B}^0\to K^-\rho^+$. CP-violating asymmetries for these decays are similar to those for $B^\pm$ decays, and no mixing is involved.

- case 2: $B^0\to(f=\bar{f})\leftarrow\overline{B}^0$, for example, $\overline{B}^0\&B^0\to\pi^0\rho^0,\eta\omega$, etc. The time-integrated asymmetries are

$$\mathcal{A}_{CP} = \frac{1}{1+x^2}a_{\epsilon'} + \frac{x}{1+x^2}a_{\epsilon+\epsilon'}, \tag{5.5}$$

$$a_{\epsilon'} = \frac{1-|\lambda_{CP}|^2}{1+|\lambda_{CP}|^2}, \quad a_{\epsilon+\epsilon'} = \frac{-2\ \mathrm{Im}(\lambda_{CP})}{1+|\lambda_{CP}|^2}, \quad \lambda_{CP} = \frac{V_{td}V_{tb}^*}{V_{td}^*V_{tb}} \frac{\mathcal{A}(\overline{B}^0(0)\to\bar{f})}{\mathcal{A}(B^0(0)\to f)}, \tag{5.6}$$

where $x = \Delta m/\Gamma = 0.73\pm0.03$ [41]. $a_{\epsilon'}$ and $a_{\epsilon+\epsilon'}$ are direct and mixing-induced CP-violating asymmetries, respectively.

- case 3: $B^0\to(f$ and $(\bar{f})\leftarrow\overline{B}^0$. There are three examples for $B\to PV$ decays; they are $\overline{B}^0$ and $B^0\to\pi^\pm\rho^\mp, K^\pm K^{*\mp}$ and $\overline{B}^0$ and $B^0\to K_S^0K^{*0}, K_S^0\overline{K}^{*0}$. We follow the conventions for the time-dependent asymmetries in [29,58]. The four basic decay amplitudes of transitions $\overline{B}^0(t)$ and $B^0(t)\to f$ and $\bar{f}$ at $t=0$ are written as

$$g = \mathcal{A}(B^0(0)\to f), \qquad \bar{g} = \mathcal{A}(\overline{B}^0(0)\to\bar{f}), \tag{5.7a}$$

$$h = \mathcal{A}(\overline{B}^0(0)\to f), \qquad \bar{h} = \mathcal{A}(B^0(0)\to\bar{f}), \tag{5.7b}$$

For example, if $f = K^+K^{*-}$, then $h$ and $\bar{g}$ will correspond to Eq.(A2) and Eq.(A6). The time-dependent decay widths are written as

$$\Gamma(B^0(t)\to f) = \frac{e^{-\Gamma t}}{2}\Big(|g|^2+|h|^2\Big)\Big[1+a_{\epsilon'}\cos(\Delta mt)+a_{\epsilon+\epsilon'}\sin(\Delta mt)\Big], \tag{5.8a}$$

$$\Gamma(\overline{B}^0(t)\to\bar{f}) = \frac{e^{-\Gamma t}}{2}\Big(|\bar{g}|^2+|\bar{h}|^2\Big)\Big[1-a_{\overline{\epsilon}'}\cos(\Delta mt)-a_{\epsilon+\overline{\epsilon}'}\sin(\Delta mt)\Big], \tag{5.8b}$$

$$\Gamma(B^0(t)\to\bar{f}) = \frac{e^{-\Gamma t}}{2}\Big(|\bar{g}|^2+|\bar{h}|^2\Big)\Big[1+a_{\overline{\epsilon}'}\cos(\Delta mt)+a_{\epsilon+\overline{\epsilon}'}\sin(\Delta mt)\Big], \tag{5.8c}$$

$$\Gamma(\overline{B}^0(t)\to f) = \frac{e^{-\Gamma t}}{2}\Big(|g|^2+|h|^2\Big)\Big[1-a_{\epsilon'}\cos(\Delta mt)-a_{\epsilon+\epsilon'}\sin(\Delta mt)\Big], \tag{5.8d}$$

where $q/p = \frac{V_{td}V_{tb}^*}{V_{td}^*V_{tb}}$, and

$$a_{\epsilon'} = \frac{|g|^2-|h|^2}{|g|^2+|h|^2}, \qquad a_{\epsilon+\epsilon'} = \frac{-2\ \mathrm{Im}[(q/p)\times(h/g)]}{1+|h/g|^2}, \tag{5.9a}$$

$$a_{\overline{\epsilon}'} = \frac{|\bar{h}|^2-|\bar{g}|^2}{|\bar{h}|^2+|\bar{g}|^2}, \qquad a_{\epsilon+\overline{\epsilon}'} = \frac{-2\ \mathrm{Im}[(q/p)\times(\bar{g}/\bar{h})]}{1+|\bar{g}/\bar{h}|^2}. \tag{5.9b}$$

Our results for CP-violating asymmetries for decays $B\to PV$ are listed in Tables VI–VIII. The parameters (including $a_{\epsilon'}$, $a_{\overline{\epsilon}'}$, $a_{\epsilon+\epsilon'}$, $a_{\epsilon+\overline{\epsilon}'}$, and $\mathcal{A}_{CP}$) with superscripts $f$ and $f+a$ are

calculated in the QCDF framework with decay amplitudes $\mathcal{A}^f(B\to PV)$ and $\mathcal{A}^f(B\to PV)+\mathcal{A}^a(B\to PV)$, respectively. Some remarks are in order.

(1) Within the QCDF framework, the strong phases are either at the order of $\alpha_s$ or power suppressed in $\Lambda_{QCD}/m_b$. Only radiative corrections are in principle calculable in the QCDF approach. However, numerically power corrections in $\Lambda_{QCD}/m_b$ might be as important as the radiative corrections. So in a sense the QCDF method can predict only the order of magnitude of the CP-violating asymmetries.

(2) The theoretical predictions for CP-violating asymmetries are compatible with measurements within one standard deviation (see Fig. 7). However, so far, the present experimental measurements on $B\to PV$ have too large uncertainties, e.g., $\mathcal{A}_{CP}(\omega\pi^\pm) = -0.34\pm0.25$ [14] or $-0.01^{+0.29}_{-0.31}\pm0.03$ [10], and $\mathcal{A}_{CP}(\phi K^\pm) = -0.05\pm0.20\pm0.03$ [10], so they cannot provide any useful information.

(3) Although the uncertainties from variations of nonperturbative parameters, such as form factors and so on, are reduced to some extent for the CP-violating asymmetries, the weak annihilations can still have great effects on the CP asymmetries for some decay channels, such as $a_{\epsilon'}$ and $a_{\epsilon+\epsilon'}$ for the $a_2$ dominant decays $\overline{B}^0\to\pi\omega,\eta\rho^0$, etc.

(4) It is worth noting that for the decays $B^0\to\phi\pi,\phi\eta^{(\prime)}$, there are no direct CP asymmetries $a_{\epsilon'}$ within the QCDF approach, while in the GF framework, $a_{\epsilon'}$ varies from $\sim$1% to $\sim$23% with $N_c^{eff}=2\sim\infty$ [29].

(5) One might wonder why the CP-violating asymmetries for the $a_1$ dominant decays $B^0\to\pi^\pm\rho^\mp$ are not as small as we expected. In fact, we only expect that the direct CP asymmetries at $t=0$ are small, i.e., $a_{\epsilon''}=\frac{|g|^2-|\bar{g}|^2}{|g|^2+|\bar{g}|^2}$ and $a_{\overline{\epsilon}''}=\frac{|h|^2-|\bar{h}|^2}{|h|^2+|h|^2}$. For instance, we take $g=\mathcal{A}(B^0\to\pi^-\rho^+)$; then with the CKM parameters in [37], $a^f_{\epsilon''}=2.3\%$, $a^{f+a}_{\epsilon''}=5.2\%$, $a^f_{\overline{\epsilon}''}=-0.2\%$ and $a^{f+a}_{\overline{\epsilon}''}=4.6\%$ at the scale $\mu=m_b$. They are really small.

## VI. CONCLUSION

(1) In the heavy quark limit, we calculated the hadronic charmless decays $B \to PV$ with the QCDF approach including chirally enhanced corrections and weak annihilation topologies. Neglecting the power suppressed $\Lambda_{QCD}/m_b$ effects, the "nonfactorizable" contributions that cannot be calculated within the NF framework are perturbatively calculable with the QCDF approach at least at the order of $\alpha_s$. They provide the strong phases which are important for CP violations.

(2) Most of the CP-averaged branching ratios are in agreement with present measurements, but there are very large theoretical uncertainties due to the variations of input parameters. However, some decay channels, such as $B \to \eta K^*$ and $B^- \to \pi^- \overline{K}^{*0}$, are only marginally consistent with the experimental observations. In these decay channels, nonperturbative contributions, such as weak annihilation topologies, play a crucial role and need further investigation.

(3) The CP asymmetries for the $a_1$ dominant decays are small because of small strong phases, $\mathcal{O}(\alpha_s)$ and/or $\mathcal{O}(\Lambda_{QCD}/m_b)$. However, the "nonfactorizable" effects and the weak annihilations can provide large imaginary parts for the $a_2$ dominant decay amplitudes, and lead to large direct CP asymmetries. The theoretical predictions for CP-violating asymmetries are compatible with current measurements within one standard deviation. It is worth noting that the QCDF predictions might give only the proper order of magnitude of the CP asymmetries.

(4) The present experimental data for nonleptonic B meson decays are not yet sufficient, especially for measurements of CP violation. On the other hand, there are still many uncertainties in the theoretical frame, for instance, the weak annihilations and other potential power corrections. Great advances in both experiment and theory in the near future are strongly expected.

## ACKNOWLEDGEMANETS

This work was Supported in part by National Natural Science Foundation of China. G. Zhu thanks JSPS of Japan for financial support. We thank Professor A. Kagan and H. Cheng for their comments on and discussions about the manuscript.


## APPENDIX A: THE ANNIHILATION AMPLITUDES FOR $B\to PV$

$$\begin{aligned}\mathcal{A}^a(\overline{B}^0\to K^0\overline{K}^{*0}) = \frac{G_F}{\sqrt{2}} f_B f_K f_{K^*}\Big\{&(V_{ub}V_{ud}^* + V_{cb}V_{cd}^*)\Big[b_3(K^0,\overline{K}^{*0})\\ &-\frac{1}{2}b_3^{ew}(K^0,\overline{K}^{*0}) + b_4(K^0,\overline{K}^{*0}) - \frac{1}{2}b_4^{ew}(K^0,\overline{K}^{*0})\\ &+b_4(\overline{K}^{*0},K^0) - \frac{1}{2}b_4^{ew}(\overline{K}^{*0},K^0)\Big]\Big\},\end{aligned} \tag{A1}$$

$$\begin{aligned}\mathcal{A}^a(\overline{B}^0\to K^+K^{*-}) = \frac{G_F}{\sqrt{2}} f_B f_K f_{K^*}\Big\{&V_{ub}V_{ud}^* b_1(K^+,K^{*-})\\ &+(V_{ub}V_{ud}^* + V_{cb}V_{cd}^*)\Big[b_4(K^+,K^{*-}) + b_4(K^{*-},K^+)\\ &+b_4^{ew}(K^+,K^{*-}) - \frac{1}{2}b_4^{ew}(K^{*-},K^+)\Big]\Big\},\end{aligned} \tag{A2}$$

$$\begin{aligned}\mathcal{A}^a(\overline{B}^0\to \pi^-\rho^+) = \frac{G_F}{\sqrt{2}} f_B f_\pi f_\rho\Big\{&V_{ub}V_{ud}^* b_1(\rho^+,\pi^-)\\ &+(V_{ub}V_{ud}^* + V_{cb}V_{cd}^*)\Big[b_3(\pi^-,\rho^+) + b_4(\rho^+,\pi^-) + b_4(\pi^-,\rho^+)\\ &-\frac{1}{2}b_3^{ew}(\pi^-,\rho^+) + b_4^{ew}(\rho^+,\pi^-) - \frac{1}{2}b_4^{ew}(\pi^-,\rho^+)\Big]\Big\},\end{aligned} \tag{A3}$$

$$\begin{aligned}\mathcal{A}^a(\overline{B}^0\to \pi^+\rho^-) = \frac{G_F}{\sqrt{2}} f_B f_\pi f_\rho\Big\{&V_{ub}V_{ud}^* b_1(\pi^+,\rho^-)\\ &+(V_{ub}V_{ud}^* + V_{cb}V_{cd}^*)\Big[b_3(\rho^-,\pi^+) + b_4(\pi^+,\rho^-) + b_4(\rho^-,\pi^+)\\ &-\frac{1}{2}b_3^{ew}(\rho^-,\pi^+) + b_4^{ew}(\pi^+,\rho^-) - \frac{1}{2}b_4^{ew}(\rho^-,\pi^+)\Big]\Big\},\end{aligned} \tag{A4}$$

$$\begin{aligned}\mathcal{A}^a(\overline{B}^0\to \pi^+K^{*-}) = \frac{G_F}{\sqrt{2}} f_B f_\pi f_{K^*}\Big\{&(V_{ub}V_{us}^* + V_{cb}V_{cs}^*)\Big[b_3(K^{*-},\pi^+)\\ &-\frac{1}{2}b_3^{ew}(K^{*-},\pi^+)\Big]\Big\},\end{aligned} \tag{A5}$$

$$\mathcal{A}^a(\overline{B}^0\to K^-K^{*+}) = \frac{G_F}{\sqrt{2}} f_B f_K f_{K^*}\Big\{ V_{ub}V_{ud}^* b_1(K^{*+},K^-) + (V_{ub}V_{ud}^* + V_{cb}V_{cd}^*)\Big[ b_4(K^{*+},K^-) + b_4(K^-,K^{*+}) + b_4^{ew}(K^{*+},K^-) - \frac{1}{2} b_4^{ew}(K^-,K^{*+})\Big]\Big\}, \tag{A6}$$

$$\mathcal{A}^a(\overline{B}^0\to K^-\rho^+) = \frac{G_F}{\sqrt{2}} f_B f_K f_\rho\Big\{ (V_{ub}V_{us}^* + V_{cb}V_{cs}^*)\Big[ b_3(K^-,\rho^+) - \frac{1}{2} b_3^{ew}(K^-,\rho^+)\Big]\Big\}, \tag{A7}$$

$$\mathcal{A}^a(\overline{B}^0\to \overline{K}^0K^{*0}) = \frac{G_F}{\sqrt{2}} f_B f_K f_{K^*}\Big\{ (V_{ub}V_{ud}^* + V_{cb}V_{cd}^*)\Big[ b_3(K^{*0},\overline{K}^0) + b_4(K^{*0},\overline{K}^0) + b_4(\overline{K}^0,K^{*0}) - \frac{1}{2} b_3^{ew}(K^{*0},\overline{K}^0) - \frac{1}{2} b_4^{ew}(K^{*0},\overline{K}^0) - \frac{1}{2} b_4^{ew}(\overline{K}^0,K^{*0})\Big]\Big\}, \tag{A8}$$

$$\mathcal{A}^a(\overline{B}^0\to \overline{K}^0\phi) = \frac{G_F}{\sqrt{2}} f_B f_K f_\phi\Big\{ (V_{ub}V_{us}^* + V_{cb}V_{cs}^*)\Big[ b_3(\phi,\overline{K}^0) - \frac{1}{2} b_3^{ew}(\phi,\overline{K}^0)\Big]\Big\}, \tag{A9}$$

$$\mathcal{A}^a(\overline{B}^0\to \overline{K}^0\rho^0) = -\frac{G_F}{2} f_B f_K f_\rho\Big\{ (V_{ub}V_{us}^* + V_{cb}V_{cs}^*)\Big[ b_3(\overline{K}^0,\rho^0) - \frac{1}{2} b_3^{ew}(\overline{K}^0,\rho^0)\Big]\Big\}, \tag{A10}$$

$$\mathcal{A}^a(\overline{B}^0\to \overline{K}^0\omega) = \frac{G_F}{2} f_B f_K f_\omega\Big\{ (V_{ub}V_{us}^* + V_{cb}V_{cs}^*)\Big[ b_3(\overline{K}^0,\omega) - \frac{1}{2} b_3^{ew}(\overline{K}^0,\omega)\Big]\Big\}, \tag{A11}$$

$$\mathcal{A}^a(\overline{B}^0\to \pi^0\rho^0) = \frac{G_F}{2\sqrt{2}} f_B f_\pi f_\rho\Big\{ V_{ub}V_{ud}^*\Big[ b_1(\rho^0,\pi^0) + b_1(\pi^0,\rho^0)\Big] + (V_{ub}V_{ud}^* + V_{cb}V_{cd}^*)\Big[ b_3(\rho^0,\pi^0) + b_3(\pi^0,\rho^0) + 2b_4(\pi^0,\rho^0) + 2b_4(\rho^0,\pi^0) - \frac{1}{2} b_3^{ew}(\rho^0,\pi^0) - \frac{1}{2} b_3^{ew}(\pi^0,\rho^0) + \frac{1}{2} b_4^{ew}(\pi^0,\rho^0) + \frac{1}{2} b_4^{ew}(\rho^0,\pi^0)\Big]\Big\}, \tag{A12}$$

$$\mathcal{A}^a(\overline{B}^0\to \pi^0\omega) = \frac{G_F}{2\sqrt{2}} f_B f_\pi f_\omega\Big\{ V_{ub}V_{ud}^*\Big[ b_1(\omega,\pi^0) + b_1(\pi^0,\omega)\Big] + (V_{ub}V_{ud}^* + V_{cb}V_{cd}^*)\Big[ - b_3(\pi^0,\omega) - b_3(\omega,\pi^0) + \frac{1}{2} b_3^{ew}(\pi^0,\omega) + \frac{1}{2} b_3^{ew}(\omega,\pi^0) + \frac{3}{2} b_4^{ew}(\pi^0,\omega) + \frac{3}{2} b_4^{ew}(\omega,\pi^0)\Big]\Big\}, \tag{A13}$$

$$\mathcal{A}^a(\overline{B}^0\to\pi^0\phi) = 0, \tag{A14}$$

$$\begin{aligned}\mathcal{A}^a(\overline{B}^0\to\pi^0\overline{K}^{*0}) = -\frac{G_F}{2} f_B f_\pi f_{K^*}\Big\{&(V_{ub}V_{us}^* + V_{cb}V_{cs}^*)\Big[b_3(\overline{K}^{*0},\pi^0)\\ &-\frac{1}{2}b_3^{ew}(\overline{K}^{*0},\pi^0)\Big]\Big\},\end{aligned} \tag{A15}$$

$$\begin{aligned}\mathcal{A}^a(\overline{B}^0\to\eta^{(\prime)}\rho^0) = \frac{G_F}{2} f_B f^u_{\eta^{(\prime)}} f_\rho\Big\{&V_{ub}V_{ud}^*\Big[b_1(\eta^{(\prime)},\rho^0) + b_1(\rho^0,\eta^{(\prime)})\Big]\\ &+(V_{ub}V_{ud}^* + V_{cb}V_{cd}^*)\Big[-b_3(\eta^{(\prime)},\rho^0) - b_3(\rho^0,\eta^{(\prime)})\\ &+\frac{1}{2}b_3^{ew}(\eta^{(\prime)},\rho^0) + \frac{1}{2}b_3^{ew}(\rho^0,\eta^{(\prime)}) + \frac{3}{2}b_4^{ew}(\eta^{(\prime)},\rho^0)\\ &+\frac{3}{2}b_4^{ew}(\rho^0,\eta^{(\prime)})\Big]\Big\},\end{aligned} \tag{A16}$$

$$\begin{aligned}\mathcal{A}^a(\overline{B}^0\to\eta^{(\prime)}\omega) = \frac{G_F}{2} f_B f^u_{\eta^{(\prime)}} f_\omega\Big\{&V_{ub}V_{ud}^*\Big[b_1(\eta^{(\prime)},\omega) + b_1(\omega,\eta^{(\prime)})\Big]\\ &+(V_{ub}V_{ud}^* + V_{cb}V_{cd}^*)\Big[b_3(\eta^{(\prime)},\omega) + b_3(\omega,\eta^{(\prime)})\\ &+2b_4(\eta^{(\prime)},\omega) + 2b_4(\omega,\eta^{(\prime)}) - \frac{1}{2}b_3^{ew}(\eta^{(\prime)},\omega)\\ &-\frac{1}{2}b_3^{ew}(\omega,\eta^{(\prime)}) + \frac{1}{2}b_4^{ew}(\eta^{(\prime)},\omega) + \frac{1}{2}b_4^{ew}(\omega,\eta^{(\prime)})\Big]\Big\},\end{aligned} \tag{A17}$$

$$\begin{aligned}\mathcal{A}^a(\overline{B}^0\to\eta^{(\prime)}\phi) = \frac{G_F}{\sqrt{2}} f_B f^s_{\eta^{(\prime)}} f_\phi\Big\{&(V_{ub}V_{ud}^* + V_{cb}V_{cd}^*)\Big[b_4(\eta^{(\prime)},\phi)\\ &+b_4(\phi,\eta^{(\prime)}) - \frac{1}{2}b_4^{ew}(\eta^{(\prime)},\phi) - \frac{1}{2}b_4^{ew}(\phi,\eta^{(\prime)})\Big]\Big\},\end{aligned} \tag{A18}$$

$$\begin{aligned}\mathcal{A}^a(\overline{B}^0\to\eta^{(\prime)}\overline{K}^{*0}) = \frac{G_F}{\sqrt{2}} f_B f^u_{\eta^{(\prime)}} f_{K^*}\Big\{&(V_{ub}V_{us}^* + V_{cb}V_{cs}^*)\Big[b_3(\overline{K}^{*0},\eta^{(\prime)})\\ &-\frac{1}{2}b_3^{ew}(\overline{K}^{*0},\eta^{(\prime)}) + \frac{f^s_{\eta^{(\prime)}}}{f^u_{\eta^{(\prime)}}}\Big(b_3(\eta^{(\prime)},\overline{K}^{*0}) - \frac{1}{2}b_3^{ew}(\eta^{(\prime)},\overline{K}^{*0})\Big)\Big]\Big\},\end{aligned} \tag{A19}$$

$$\begin{aligned}\mathcal{A}^a(B^-\to K^0K^{*-}) = \frac{G_F}{\sqrt{2}} f_B f_K f_{K^*}\Big\{&V_{ub}V_{ud}^* b_2(K^0,K^{*-})\\ &+(V_{ub}V_{ud}^* + V_{cb}V_{cd}^*)\Big[b_3(K^0,K^{*-}) + b_3^{ew}(K^0,K^{*-})\Big]\Big\},\end{aligned} \tag{A20}$$

$$\begin{aligned}\mathcal{A}^a(B^-\to\pi^-\rho^0) = \frac{G_F}{2} f_B f_\pi f_\rho\Big\{&V_{ub}V_{ud}^*\Big[b_2(\pi^-,\rho^0) - b_2(\rho^0,\pi^-)\Big]\\ &+(V_{ub}V_{ud}^* + V_{cb}V_{cd}^*)\Big[b_3(\pi^-,\rho^0) - b_3(\rho^0,\pi^-)\\ &+b_3^{ew}(\pi^-,\rho^0) - b_3^{ew}(\rho^0,\pi^-)\Big]\Big\},\end{aligned} \tag{A21}$$

$$\mathcal{A}^a(B^-\to\pi^-\omega) = \frac{G_F}{2} f_B f_\pi f_\omega \Big\{ V_{ub}V_{ud}^* \Big[ b_2(\pi^-,\omega) + b_2(\omega,\pi^-) \Big] + (V_{ub}V_{ud}^* + V_{cb}V_{cd}^*) \Big[ b_3(\pi^-,\omega) + b_3(\omega,\pi^-) + b_3^{ew}(\pi^-,\omega) + b_3^{ew}(\omega,\pi^-) \Big] \Big\}, \tag{A22}$$

$$\mathcal{A}^a(B^-\to\pi^-\phi) = 0, \tag{A23}$$

$$\mathcal{A}^a(B^-\to\pi^-\overline{K}^{*0}) = \frac{G_F}{\sqrt{2}} f_B f_\pi f_{K^*} \Big\{ V_{ub}V_{us}^* b_2(\overline{K}^{*0},\pi^-) + (V_{ub}V_{us}^* + V_{cb}V_{cs}^*) \Big[ b_3(\overline{K}^{*0},\pi^-) + b_3^{ew}(\overline{K}^{*0},\pi^-) \Big] \Big\}, \tag{A24}$$

$$\mathcal{A}^a(B^-\to\pi^0\rho^-) = \frac{G_F}{2} f_B f_\pi f_\rho \Big\{ V_{ub}V_{ud}^* \Big[ b_2(\rho^-,\pi^0) - b_2(\pi^0,\rho^-) \Big] + (V_{ub}V_{ud}^* + V_{cb}V_{cd}^*) \Big[ b_3(\rho^-,\pi^0) - b_3(\pi^0,\rho^-) + b_3^{ew}(\rho^-,\pi^0) - b_3^{ew}(\pi^0,\rho^-) \Big] \Big\}, \tag{A25}$$

$$\mathcal{A}^a(B^-\to\pi^0K^{*-}) = \frac{G_F}{2} f_B f_\pi f_{K^*} \Big\{ V_{ub}V_{us}^* b_2(K^{*-},\pi^0) + (V_{ub}V_{us}^* + V_{cb}V_{cs}^*) \Big[ b_3(K^{*-},\pi^0) + b_3^{ew}(K^{*-},\pi^0) \Big] \Big\}, \tag{A26}$$

$$\mathcal{A}^a(B^-\to\eta^{(\prime)}\rho^-) = \frac{G_F}{\sqrt{2}} f_B f^u_{\eta^{(\prime)}} f_\rho \Big\{ V_{ub}V_{ud}^* \Big[ b_2(\rho^-,\eta^{(\prime)}) + b_2(\eta^{(\prime)},\rho^-) \Big] + (V_{ub}V_{ud}^* + V_{cb}V_{cd}^*) \Big[ b_3(\rho^-,\eta^{(\prime)}) + b_3(\eta^{(\prime)},\rho^-) + b_3^{ew}(\rho^-,\eta^{(\prime)}) + b_3^{ew}(\eta^{(\prime)},\rho^-) \Big] \Big\}, \tag{A27}$$

$$\mathcal{A}^a(B^-\to\eta^{(\prime)}K^{*-}) = \frac{G_F}{\sqrt{2}} f_B f^u_{\eta^{(\prime)}} f_{K^*} \Big\{ V_{ub}V_{us}^* \Big[ b_2(K^{*-},\eta^{(\prime)}) + \frac{f^s_{\eta^{(\prime)}}}{f^u_{\eta^{(\prime)}}} b_2(\eta^{(\prime)},K^{*-}) \Big] + (V_{ub}V_{us}^* + V_{cb}V_{cs}^*) \Big[ b_3(K^{*-},\eta^{(\prime)}) + b_3^{ew}(K^{*-},\eta^{(\prime)}) + \frac{f^s_{\eta^{(\prime)}}}{f^u_{\eta^{(\prime)}}} \Big( b_3(\eta^{(\prime)},K^{*-}) + b_3^{ew}(\eta^{(\prime)},K^{*-}) \Big) \Big] \Big\}, \tag{A28}$$

$$\mathcal{A}^a(B^-\to K^-K^{*0}) = \frac{G_F}{\sqrt{2}} f_B f_K f_{K^*} \Big\{ V_{ub}V_{ud}^* b_2(K^{*0},K^-) + (V_{ub}V_{ud}^* + V_{cb}V_{cd}^*) \Big[ b_3(K^{*0},K^-) + b_3^{ew}(K^{*0},K^-) \Big] \Big\}, \tag{A29}$$

$$\mathcal{A}^a(B^-\to K^-\phi) = \frac{G_F}{\sqrt{2}} f_B f_K f_\phi \Big\{ V_{ub}V_{us}^* b_2(\phi, K^-) + (V_{ub}V_{us}^* + V_{cb}V_{cs}^*)\Big[b_3(\phi, K^-) + b_3^{ew}(\phi, K^-)\Big]\Big\}, \tag{A30}$$

$$\mathcal{A}^a(B^-\to K^-\omega) = \frac{G_F}{2} f_B f_K f_\omega \Big\{ V_{ub}V_{us}^* b_2(K^-, \omega) + (V_{ub}V_{us}^* + V_{cb}V_{cs}^*)\Big[b_3(K^-, \omega) + b_3^{ew}(K^-, \omega)\Big]\Big\}, \tag{A31}$$

$$\mathcal{A}^a(B^-\to K^-\rho^0) = \frac{G_F}{2} f_B f_K f_\rho \Big\{ V_{ub}V_{us}^* b_2(K^-, \rho^0) + (V_{ub}V_{us}^* + V_{cb}V_{cs}^*)\Big[b_3(K^-, \rho^0) + b_3^{ew}(K^-, \rho^0)\Big]\Big\}, \tag{A32}$$

$$\mathcal{A}^a(B^-\to \overline{K}^0\rho^-) = \frac{G_F}{\sqrt{2}} f_B f_K f_\rho \Big\{ V_{ub}V_{us}^* b_2(\overline{K}^0, \rho^-) + (V_{ub}V_{us}^* + V_{cb}V_{cs}^*)\Big[b_3(\overline{K}^0, \rho^-) + b_3^{ew}(\overline{K}^0, \rho^-)\Big]\Big\}. \tag{A33}$$

# REFERENCES


[1] A. Bozek (for the Belle Collaboration), in *Proceedings of the 4th International Conference on B Physics & CP Violation, Ise-Shima, Japan, February, 2001*, hep-ex/0104041.

[2] K. Abe, *et al.* (for the Belle Collaboration), hep-ex/0201007.

[3] K. Abe, *et al.* (for the Belle Collaboration), Belle-CONF-0115 (2001), in *Proceedings of the XX International Symposium on Lepton & Photon Interactions at High Energies, July 23-28, 2001, Rome, Italy.*

[4] H. Tajima (for the Belle Collaboration), hep-ex/0111037.

[5] B. Aubert, *et al.* (for the BABAR Collaboration), Phys.Rev.Lett.**87**, 151801 (2001) .

[6] Thomas Schietinger (for the BABAR Collaboration), in *Proceedings of the Lake Louise Winter Institute on Fundamental Interactions, Alberta, Canada, February, 2001* hep-ex/0105019.

[7] B. Aubert, *et al.* (for the BABAR Collaboration), hep-ex/0107037.

[8] B. Aubert, *et al.* (for the BABAR Collaboration), hep-ex/0107058.

[9] B. Aubert, *et al.* (for the BABAR COllaboration), Phys.Rev.Lett.**87**, 221802 (2001).

[10] B. Aubert, *et al.* (for the BABAR COllaboration), hep-ex/0109006.

[11] B. Aubert, *et al.* (for the BABAR COllaboration), hep-ex/0109007.

[12] M. Bishai, *et al.* (CLEO Collaboration), hep-ex/9908018

[13] S. J. Richichi, *et al.* (CLEO Collaboration), Phys.Rev.Lett.**85**, 520 (2000).

[14] S. Chen, *et al.* (CLEO Collaboration), Phys.Rev.Lett.**85**, 525 (2000).

[15] C. P. Jessop, *et al.* (CLEO Collaboration), Phys.Rev.Lett.**85**, 2881 (2000).

[16] R. A. Briere, *et al.* (CLEO Collaboration), Phys.Rev.Lett.**86**, 3718 (2001).

[17] For a review, see G. Buchalla, A. J. Buras and M. E. Lautenbacher, Rev.Mod.Phys.**68**, 1125 (1996); or A. J. Buras, hep-ph/9806471.

[18] M. Bauer and B. Stech, Phys.Lett.**B152**, 380 (1985); M. Wirbel, B. Stech, and M. Bauer, Z.Phys.**C29**, 637 (1985); M. Bauer, B. Stech, and M. Wirbel, Z.Phys.**C34**, 103 (1987).

[19] J. D. Bjorken, Nucl.Phys.(Proc.Suppl.)**B11**, 325 (1989).

[20] H. Y. Cheng and K. C. Yang, Phys.Rev.**D62**, 054029 (2000).

[21] M. Beneke, G. Buchalla, M. Neubert and C. T. Sachrajda, Phys.Rev.Lett.**83**, 1914 (1999); Nucl.Phys.**B591**, 313 (2000).

[22] M. Beneke, G. Buchalla, M. Neubert and C. T. Sachrajda, Nucl.Phys.**B606**, 245 (2001).

[23] H. Y. Cheng and K. C. Yang, Phys.Lett.**B511**, 40 (2001).

[24] H. Y. Cheng and K. C. Yang, Phys.Rev.**D64**, 074004 (2001).

[25] M. Z. Yang and Y. D. Yang, Phys.Rev.**D62**, 114019 (2000).

[26] T. Muta, A. Sugamoto, M. Z. Yang and Y. D. Yang, Phys.Rev.**D62**, 094020 (2000).

[27] D. S. Du, D. S. Yang and G. H. Zhu, Phys.Rev.**D64**, 014036 (2001); Phys.Lett.**B509**, 263-272 (2001); Phys.Lett.**B488**, 46-54 (2000);

[28] D. S. Du, H. J. Gong, J. F. Sun, D. S. Yang and G. H. Zhu, Phys.Rev.**D65**, 074001 (2002).

[29] A. Ali, G. Kramer and C. D. Lü, Phys.Rev.**D58**, 094009 (1998); Phys.Rev.**D59**, 014005 (1999).

[30] Y. H. Chen, H. Y. Cheng, B. Tseng and K. C. Yang, Phys.Rev.**D60**, 094014 (1999).

[31] C. D. Lü and M. Z. Yang, Eur.Phys.J.**C23**, 275 (2002).

[32] S. Descotes, C. T. Sachrajda, Nucl.Phys.**B625**, 239 (2002).

[33] L. Wolfenstein, Phys.Rev.Lett.**51**, 1945 (1983).

[34] Y. Y. Keum, H. N. Li and A. I. Sanda, Phys.Lett.**B504**, 6 (2001); Phys.Rev.**D63**, 054008 (2001); Y.Y. Keum, H. N. Li, Phys.Rev.**D63**, 074006 (2001).

[35] C. D. Lü, K. Ukai and M. Z. Yang, Phys.Rev.**D63**, 074009 (2001).

[36] M. Ciuchini, *et al.* J.High Energy Phys. **07**, 013 (2001).

[37] M. Ciuchini, hep-ph/0112133.

[38] A. Höcker, H. Lacker, S. Laplace, and F. Le Diberder, Eur.Phys.J.**C21**, 225-259 (2001); for an update, see http://www.slac.stanford.edu/˜laplace/ckmfitter.html .

[39] M. Nubert, hep-ph/0110301; or refer to H. Lacker, "*Implementing theoretical calculations for $B\to\pi\pi/K\pi$ in CkmFitter*", July 20, 2001 at Regensburg, Germany.

[40] P. Colangelo and A. Khodjamirian, hep-ph/0010175.

[41] D. Croone *et al.* (Particle Data Group), Eur.Phys.J.**C15**, 1 (2000).

[42] H. Leutwyler, Nucl.Phys.Proc.Suppl.**64**, 223 (1998).

[43] P. Herrera-Siklódy, J. I. Latorre, P. Pascual and J. Taron, Phys.Lett.**B419**, 326 (1998).

[44] J. M. Flynn, *et al.* (for the UKQCD Collaboration), Nucl.Phys.**B461**, 327 (1996).

[45] A. Khodjamirian, *et al.* Phys.Rev.**D62**, 114002 (2000).

[46] P. Ball, J. High Energy Phys. **09**, 005 (1998).

[47] A. Ali, V. M. Braun and H. Simma, Z.Phys.**C63**, 437 (1994).

[48] V. M. Braun and I. E. Filyanov, Z.Phys.**C44**, 157 (1989); Z.Phys.**C48**, 239 (1990).

[49] P. Ball and V.M. Braun, Nucl.Phys.**B543**, 201 (1999); hep-ph/9808229.

[50] M. Bauer and M. Wirbel, Z.Phys.C **42**,671 (1989).

[51] X. G. He, J. P. Ma and C. Y. Wu, Phys.Rev.**D63**, 094004 (2001).

[52] I. Halperin and A. Zhitnitsky, Phys.Rev.**D56**, 7247 (1997).

[53] A. Ali and C. Greub, Phys.Rev.**D57**, 2996 (1998).

[54] A. Ali, J. Chay, C. Greub and P. Ko, Phys.Lett.**B424**, 161 (1998).

[55] D. S. Du, C. S. Kim and Y. D. Yang, Phys.Lett.**B426**, 133 (1998).

[56] M. R. Ahmady, E. Kou and A. Sugamoto, Phys.Rev.**D58**, 014015 (1998).

[57] M. Z. Yang and Y. D. Yang, Nucl.Phys.**B609**, 469 (2001).

[58] W. F. Palmer and Y. L. Wu, Phys.Lett.**B350**, 245 (1995).

## FIGURES

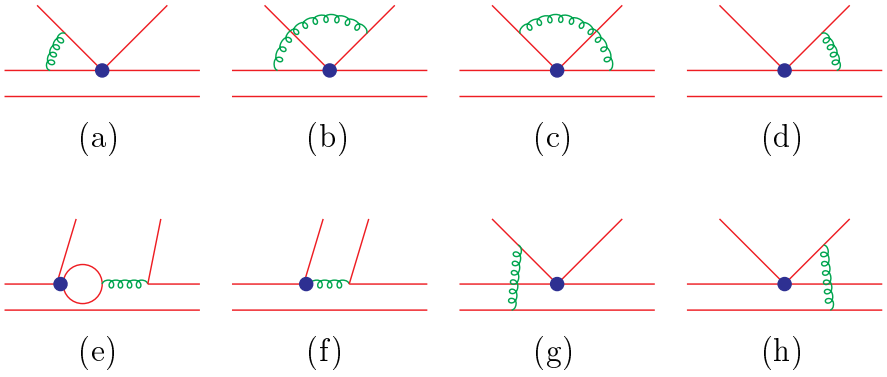


FIG. 1. Order of $\alpha_s$ corrections to the hard-scattering kernels. The upward quark lines represent the emitted mesons from b quark weak decays. These diagrams are commonly called vertex corrections, penguin corrections, and hard spectator scattering diagrams for Fig.(a-d), Fig.(e-f), and Fig.(g-h) respectively.

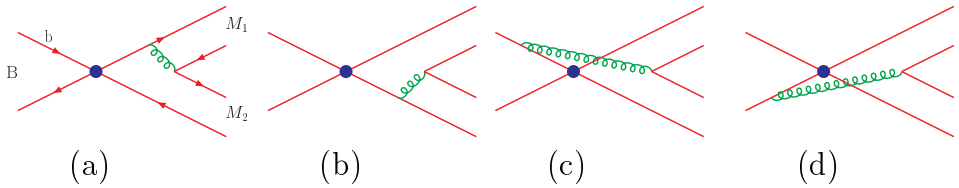


FIG. 2. Order of $\alpha_s$ corrections to the weak annihilations of charmless decays $B \to PV$.

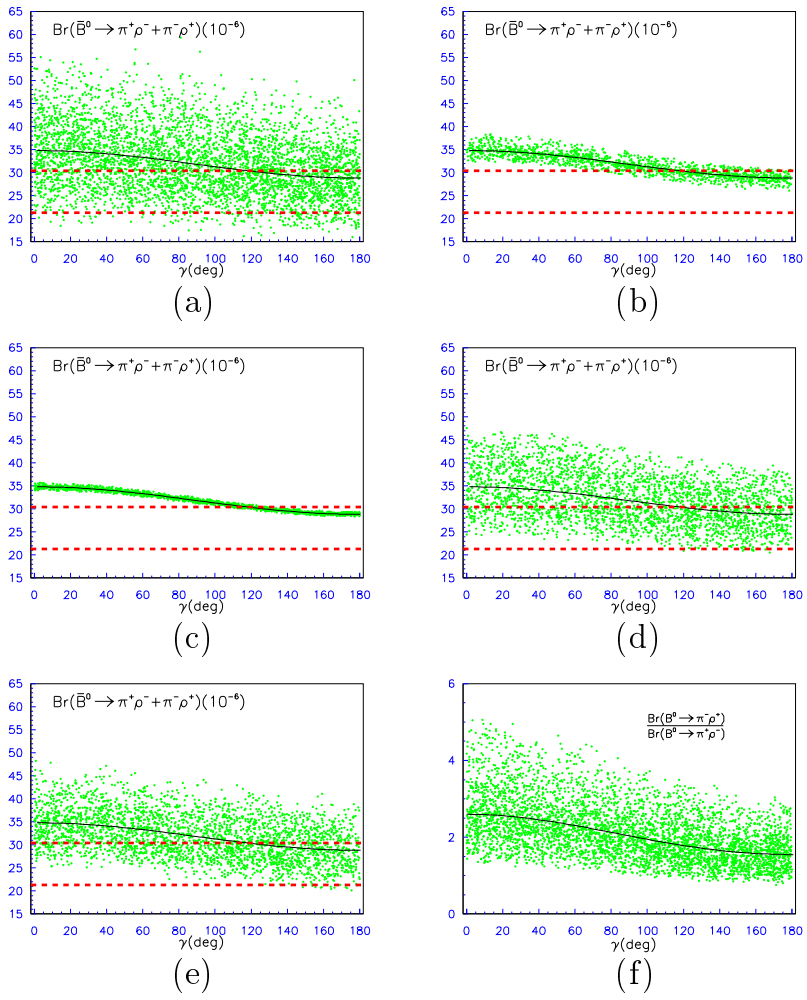


FIG. 3. Decays $\overline{B}^0$ and $B^0 \to \pi^\pm\rho^\mp$ versus $\gamma$ at the scale $\mu = m_b$ within the QCDF approach, including the effects of weak annihilations. Fig.(a-e) are CP-averaged branching ratios, and Fig.(f) is the ratio $\frac{\mathcal{B}r(B^0 \to \pi^-\rho^+)}{\mathcal{B}r(B^0 \to \pi^+\rho^-)}$. The solid lines are drawn with central values of various parameters; the bands between the dashed lines denote measurement within $1\sigma$. The shaded dots originate from uncertainties due to variations of parameters, such as in Fig.(b) due to $X_A$, in Fig.(c) due to $X_H$, in Fig.(d) due to form factors, in Fig.(e) due to CKM elements, and in Fig.(a,f) due to various parameters.

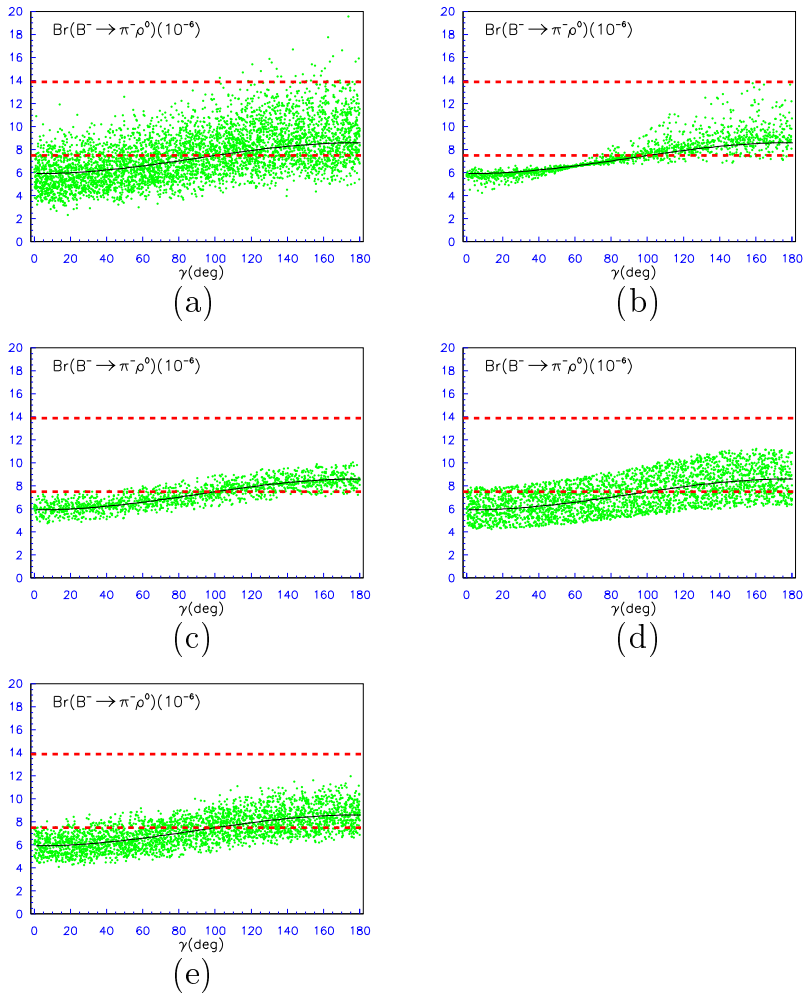


FIG. 4. $\mathcal{B}r(B^-\to\pi^-\rho^0)$ versus $\gamma$ at the scale $\mu = m_b$ with the QCDF approach, including the weak annihilation contributions. The solid lines are drawn with the default values of various parameters; the bands between the dashed lines denote averaged measurement within $1\sigma$. The shaded dots demonstrate the uncertainties due to variations of various parameters in Fig.(a), $X_A$ in Fig.(b), $X_H$ in Fig.(c), form factors in Fig.(d), and CKM matrix elements in Fig.(e).

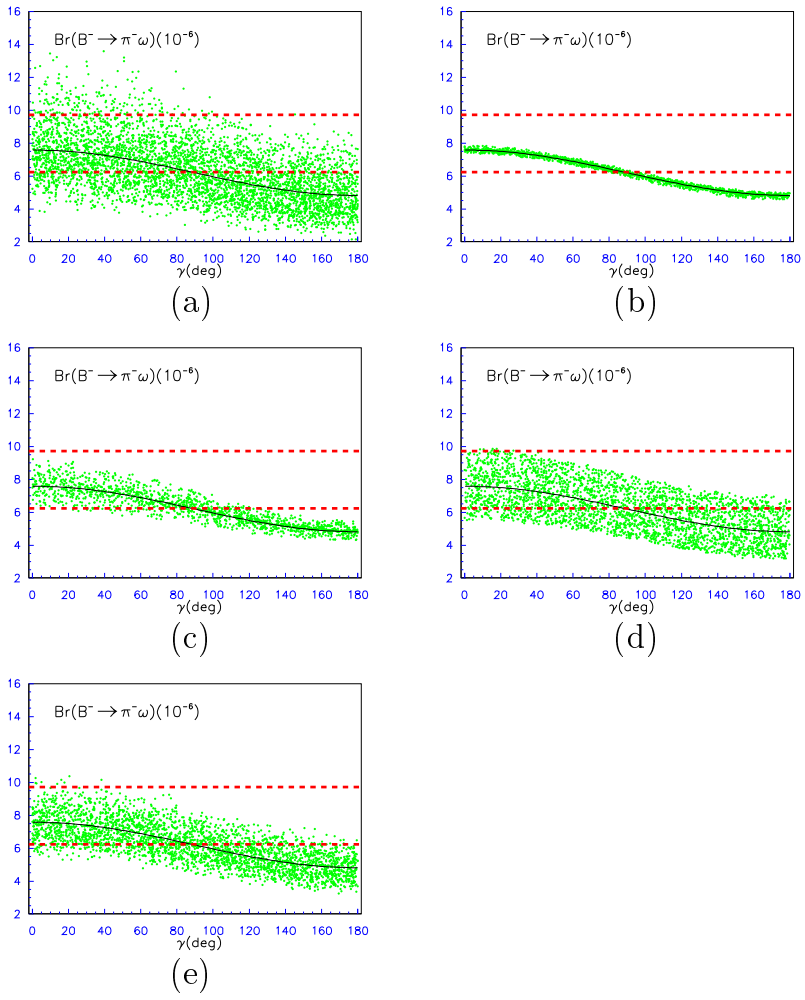


FIG. 5. $\mathcal{B}r(B^-\to\pi^-\omega)$ versus $\gamma$ at the scale $\mu = m_b$ with the QCDF approach, including the weak annihilation contributions. The meaning of the solid lines, the bands, and shaded dots is the same as in Fig.4.

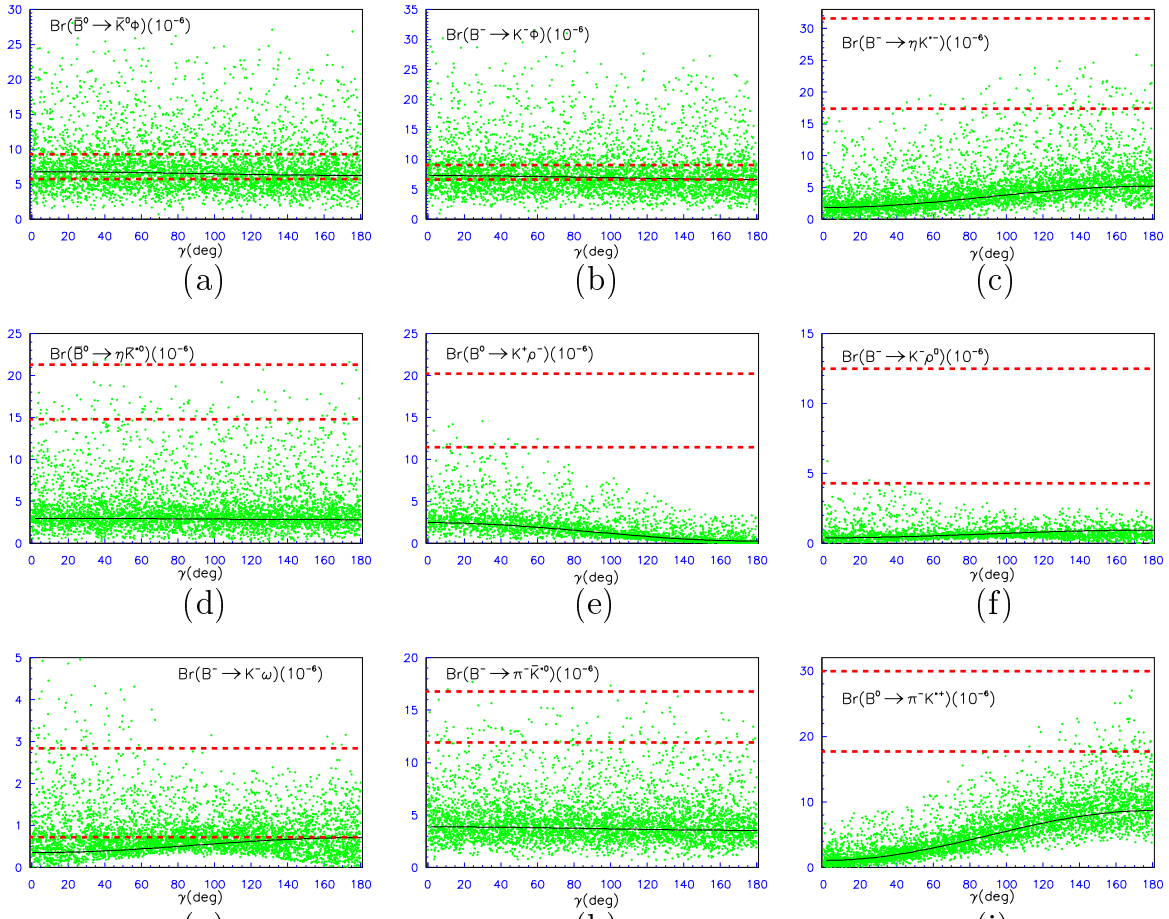


FIG. 6. The CP-averaged branching ratios of $B \to PV$ versus $\gamma$ at the scale $\mu = m_b$ with the QCDF approach, including the weak annihilation contributions. The meanings of the solid lines and bands are the same as in Fig.4. The shaded dots denote the uncertainties due to variations of various parameters.

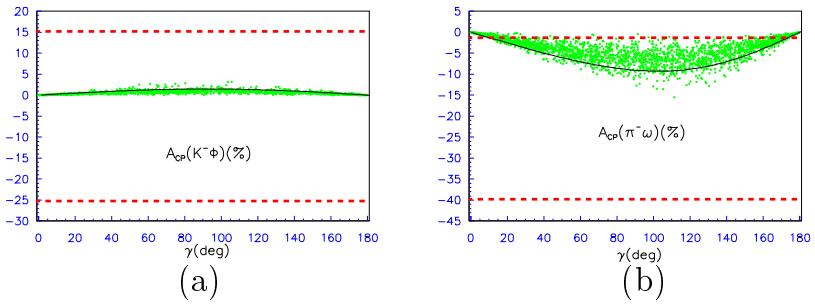


FIG. 7. CP-violating asymmetries $\mathcal{A}_{CP}(B^{\pm} \to K^{\pm}\phi)$ in Fig.(a) and $\mathcal{A}_{CP}(B^{\pm} \to \pi^{\pm}\omega)$ in Fig.(b) versus $\gamma$ at the scale $\mu = m_b$ with the QCDF approach, including the effects of weak annihilations. The meanings of the solid lines, bands, and shaded dots are the same as in Fig.4.

## TABLES

TABLE I. Wilson coefficients in NDR scheme. The input parameters in numerical calculations are fixed as $\alpha_s(m_Z) = 0.1185$, $\alpha_{em}(m_W) = 1/128$, $m_W = 80.42\text{GeV}$, $m_Z = 91.188\text{GeV}$, $m_t = 168.2\text{GeV}$, $m_b = 4.6\text{GeV}$.

| | $\mu = m_b/2$ | | $\mu = m_b$ | | $\mu = 2m_b$ | |
|---|---|---|---|---|---|---|
| | NLO | LO | NLO | LO | NLO | LO |
| $C_1$ | 1.136 | 1.178 | 1.080 | 1.115 | 1.044 | 1.073 |
| $C_2$ | -0.283 | -0.353 | -0.181 | -0.245 | -0.105 | -0.165 |
| $C_3$ | 0.021 | 0.020 | 0.014 | 0.012 | 0.009 | 0.008 |
| $C_4$ | -0.050 | -0.048 | -0.035 | -0.033 | -0.024 | -0.023 |
| $C_5$ | 0.010 | 0.010 | 0.009 | 0.008 | 0.007 | 0.006 |
| $C_6$ | -0.063 | -0.061 | -0.041 | -0.038 | -0.026 | -0.024 |
| $C_7/\alpha_{em}$ | -0.020 | -0.103 | -0.004 | -0.096 | 0.019 | -0.081 |
| $C_8/\alpha_{em}$ | 0.082 | 0.024 | 0.052 | 0.015 | 0.033 | 0.010 |
| $C_9/\alpha_{em}$ | -1.339 | -0.089 | -1.263 | -0.086 | -1.201 | -0.074 |
| $C_{10}/\alpha_{em}$ | 0.369 | -0.022 | 0.253 | -0.016 | 0.168 | -0.012 |
| $C_{7\gamma}$ | | -0.341 | | -0.304 | | -0.272 |
| $C_{8g}$ | | -0.160 | | -0.145 | | -0.132 |

TABLE II. Numerical values of coefficients $a_{i,I}$ with the default values of various parameters for case I (the recoiled mesons $M_1$ are vector mesons, and the emitted mesons $M_2$ are pseudoscalar mesons).

| | $\mu = m_b/2$ | $\mu = m_b$ | $\mu = 2m_b$ |
|---|---|---|---|
| $a_{1,I}$ | 1.077+0.033i | 1.055+0.018i | 1.038+0.010i |
| $a_{2,I}$ | -0.023-0.110i | 0.018-0.082i | 0.057-0.065i |
| $a_{3,I}(10^{-4})$ | 91.649+44.722i | 70.951+24.259i | 49.938+14.036i |
| $a^u_{4,I}(10^{-4})$ | -331.4-188.31i | -299.26-152.67i | -270.97-129.36i |
| $a^c_{4,I}(10^{-4})$ | -406.48-60.422i | -355.33-57.162i | -315.76-53.065i |
| $a_{5,I}(10^{-4})$ | -99.038-56.834i | -65.932-27.934i | -39.693-14.646i |
| $a^u_{6,I}(10^{-4})$ | -558.53-169.85i | -416.46-143.94i | -327.55-124.53i |
| $a^c_{6,I}(10^{-4})$ | -600.85-40.033i | -448.06-46.988i | -352.8- 47.08i |
| $a^u_{6,I}r_\chi(10^{-4})$ | -484.0-147.19i | -483.15-166.99i | -474.92-180.56i |
| $a^c_{6,I}r_\chi(10^{-4})$ | -520.68-34.691i | -519.81-54.512i | -511.53-68.263i |
| $a_{7,I}(10^{-4})$ | 0.539+0.175i | 1.101+0.086i | 2.419+0.048i |
| $a^u_{8,I}(10^{-4})$ | 7.383-0.330i | 4.759-0.803i | 2.934-1.165i |
| $a^c_{8,I}(10^{-4})$ | 7.344-0.209i | 4.632-0.415i | 2.741-0.574i |
| $a^u_{8,I}r_\chi(10^{-4})$ | 6.398-0.286i | 5.521-0.932i | 4.254-1.689i |
| $a^c_{8,I}r_\chi(10^{-4})$ | 6.364-0.181i | 5.374-0.481i | 3.974-0.832i |
| $a_{9,I}(10^{-4})$ | -94.827+0.160i | -91.903+0.092i | -89.29+0.057i |
| $a^u_{10,I}(10^{-4})$ | -2.426+0.318i | -9.989-0.309i | -15.972-0.812i |
| $a^c_{10,I}(10^{-4})$ | -2.497+0.438i | -10.214+0.073i | -16.314-0.230i |

TABLE III. Summary of experimental data for the branching ratios (in units of $10^{-6}$) for several charmless hadronic $B \to PV$. Inequality denotes 90% C.L. upper limits. The last column is for the averages of the uncorrelated measurements

| decay decay | BaBar | Belle | CLEO | Averaged |
|---|---|---|---|---|
| $\overline{B}^0 \to \pi^\mp \rho^\pm$ | $28.9 \pm 5.4 \pm 4.3$ [8] | $20.2^{+8.3}_{-6.6} \pm 3.3$ [1] | $27.6^{+8.4}_{-7.4} \pm 4.2$ [15] | $25.9 \pm 4.5$ |
| | | $(< 35.7)$ | | |
| $B^- \to \pi^- \rho^0$ | $< 39$ [6] | $11.2^{+5.3}_{-4.8} \pm 1.9$ [1] | $10.4^{+3.3}_{-3.4} \pm 2.1$ [15] | $10.7 \pm 3.2$ |
| | | $(< 28.8)$ | | |
| $B^- \to \pi^- \omega$ | $6.6^{+2.1}_{-1.8} \pm 0.7$ [9] | $< 9.4$ [1] | $11.3^{+3.3}_{-2.9} \pm 1.4$ [15] | $8.0 \pm 1.7$ |
| $\overline{B}^0 \to K^- \rho^+$ | | $15.8^{+5.1+1.7}_{-4.6-3.0}$ [3] | $16.0^{+7.6}_{-6.4} \pm 2.8$ [15] | $15.9 \pm 4.4$ |
| | | | $(< 32)$ | |
| $\overline{B}^0 \to \overline{K}^0 \omega$ | $6.4^{+3.6}_{-2.8} \pm 0.8$ [9] | | $10.0^{+5.4}_{-4.2} \pm 1.4$ [15] | $7.5 \pm 2.8$ |
| | $(< 13)$ | | $(< 21)$ | |
| $\overline{B}^0 \to \overline{K}^0 \phi$ | $8.1^{+3.1}_{-2.5} \pm 0.8$ [5] | $8.9^{+3.4}_{-2.7} \pm 1.0$ [4] | $5.4^{+3.7}_{-2.7} \pm 0.7$ [16] | $7.5 \pm 1.8$ |
| | | | $(< 12.3)$ | |
| $\overline{B}^0 \to \eta \overline{K}^{*0}$ | $19.8^{+6.5}_{-5.6} \pm 1.7$ [7] | $21.2^{+5.4}_{-4.7} \pm 2.0$ [4] | $13.8^{+5.5}_{-4.6} \pm 1.6$ [13] | $18.0 \pm 3.2$ |
| $B^- \to \pi^- \overline{K}^{*0}$ | $15.5 \pm 3.4 \pm 1.8$ [11] | $19.4^{+4.2+2.1+3.5}_{-3.9-2.1-6.8}$ [2] | $7.6^{+3.5}_{-3.0} \pm 1.6$ [15] | $14.3 \pm 2.4$ |
| | | | $(< 16)$ | |
| $B^- \to \eta K^{*-}$ | $22.1^{+11.1}_{-9.2} \pm 3.3$ [7] | | $26.4^{+9.6}_{-8.2} \pm 3.3$ [13] | $24.5 \pm 7.1$ |
| | $(< 33.9)$ | | | |
| $B^- \to K^- \rho^0$ | $< 29$ [6] | $< 13.5$ [1] | $8.4^{+4.0}_{-3.4} \pm 1.8$ [15] | $8.4 \pm 4.1$ |
| | | | $(< 17)$ | |
| $B^- \to K^- \omega$ | $1.4^{+1.3}_{-1.0} \pm 0.3$ [9] | $< 10.5$ [1] | $3.2^{+2.4}_{-1.9} \pm 0.8$ [15] | $1.8 \pm 1.1$ |
| | $(< 4)$ | | $(< 7.9)$ | |
| $B^- \to K^- \phi$ | $7.7^{+1.6}_{-1.4} \pm 0.8$ [5] | $11.2^{+2.2}_{-2.0} \pm 1.4$ [4] | $5.5^{+2.1}_{-1.8} \pm 0.6$ [16] | $7.9 \pm 1.2$ |
| $\overline{B}^0 \to \pi^+ K^{*-}$ | | $26.0 \pm 8.3 \pm 3.5$ [3] | $22^{+8+4}_{-6-5}$ [12] | $23.8 \pm 6.1$ |

TABLE IV. CP-averaged branching ratios (in units of $10^{-6}$) of decays $B\to PV$ for $b\to d$ transitions with central values of various parameters. The results in columns 2∼4 are calculated with $A=0.819$, $\lambda=0.2237$, $\bar{\rho}=0.218$, and $\bar{\eta}=0.316$, while the results in columes 5∼7 are computed with $A=0.83$, $\lambda=0.222$, $\bar{\rho}=0.05$, and $\bar{\eta}=0.381$.

| decay | NF | QCDF | | NF | QCDF | | |
|---|---|---|---|---|---|---|---|
| modes | $\mathcal{B}r$ | $\mathcal{B}r^f$ | $\mathcal{B}r^{f+a}$ | $\mathcal{B}r$ | $\mathcal{B}r^f$ | $\mathcal{B}r^{f+a}$ | Exp. |
| $\overline{B}^0\to K^0\overline{K}^{*0}$ | 0.023 | 0.034 | 0.040 | 0.034 | 0.050 | 0.061 | — |
| $\overline{B}^0\to \overline{K}^0 K^{*0}$ | 0.132 | 0.198 | 0.210 | 0.191 | 0.270 | 0.293 | — |
| $\overline{B}^0\to K^{\pm}K^{*\mp}$ | — | — | 0.019 | — | — | 0.019 | — |
| $\overline{B}^0\to \pi^-\rho^+$ | 9.231 | 9.685 | 10.13 | 9.31 | 9.836 | 10.28 | see Tab.III |
| $\overline{B}^0\to \pi^+\rho^-$ | 21.59 | 22.72 | 23.36 | 19.8 | 20.70 | 21.34 | see Tab.III |
| $\overline{B}^0\to \pi^0\rho^0$ | 0.452 | 0.132 | 0.139 | 0.434 | 0.124 | 0.127 | $<5.5$ [15] |
| $\overline{B}^0\to \pi^0\omega$ | 0.022 | 0.035 | 0.022 | 0.016 | 0.027 | 0.027 | $<3$ [9] |
| $\overline{B}^0\to \pi^0\phi$ | 0.0003 | 0.0006 | — | 0.0004 | 0.0008 | — | $<5$ [41] |
| $\overline{B}^0\to \eta\rho^0$ | 0.002 | 0.010 | 0.037 | 0.004 | 0.014 | 0.042 | $<10$ [41] |
| $\overline{B}^0\to \eta'\rho^0$ | 0.009 | 0.019 | 0.040 | 0.007 | 0.016 | 0.030 | $<12$ [41] |
| $\overline{B}^0\to \eta\omega$ | 0.253 | 0.113 | 0.129 | 0.206 | 0.092 | 0.100 | $<12$ [41] |
| $\overline{B}^0\to \eta'\omega$ | 0.161 | 0.061 | 0.068 | 0.162 | 0.063 | 0.072 | $<60$ [41] |
| $\overline{B}^0\to \eta\phi$ | 0.0001 | 0.0004 | 0.0005 | 0.0002 | 0.0006 | 0.0007 | $<9$ [41] |
| $\overline{B}^0\to \eta'\phi$ | 0.0001 | 0.0003 | 0.0002 | 0.0001 | 0.0004 | 0.0003 | $<31$ [41] |
| $B^-\to \pi^-\rho^0$ | 7.758 | 6.464 | 6.498 | 8.125 | 6.949 | 6.954 | see Tab.III |
| $B^-\to \pi^-\omega$ | 7.988 | 7.08 | 6.977 | 7.292 | 6.349 | 6.260 | see Tab.III |
| $B^-\to \pi^-\phi$ | 0.0006 | 0.0012 | — | 0.0009 | 0.0017 | — | $<5$ [41] |
| $B^-\to \pi^0\rho^-$ | 14.64 | 13.55 | 13.54 | 13.05 | 11.91 | 11.97 | $<43$ [15] |
| $B^-\to \eta\rho^-$ | 6.627 | 5.879 | 5.798 | 6.197 | 5.489 | 5.415 | $<15$ [13] |
| $B^-\to \eta'\rho^-$ | 4.954 | 4.424 | 4.366 | 4.935 | 4.494 | 4.438 | $<33$ [13] |
| $B^-\to K^0K^{*-}$ | 0.025 | 0.036 | 0.045 | 0.036 | 0.054 | 0.061 | — |

| | | | | | | | |
|---|---|---|---|---|---|---|---|
| $B^-\to K^-K^{*0}$ | 0.141 | 0.20 | 0.211 | 0.204 | 0.274 | 0.311 | $< 5.3$ [15] |

TABLE V. CP-averaged branching ratios (in units of $10^{-6}$) of decays $B\to PV$ for $b\to s$ transitions with central values of various parameters. The results in columns 2∼4 are calculated with $A = 0.819$, $\lambda = 0.2237$, $\bar{\rho} = 0.218$, and $\bar{\eta} = 0.316$, while the results in columns 5∼7 are computed with $A = 0.83$, $\lambda = 0.222$, $\bar{\rho} = 0.05$, and $\bar{\eta} = 0.381$.

| decay | NF | QCDF | | NF | QCDF | | |
|---|---|---|---|---|---|---|---|
| modes | $\mathcal{B}r$ | $\mathcal{B}r^f$ | $\mathcal{B}r^{f+a}$ | $\mathcal{B}r$ | $\mathcal{B}r^f$ | $\mathcal{B}r^{f+a}$ | Exp. |
| $\overline{B}^0\to K^-\rho^+$ | 1.485 | 1.848 | 2.008 | 1.081 | 1.321 | 1.501 | see Tab.III |
| $\overline{B}^0\to \overline{K}^0\rho^0$ | 0.918 | 1.184 | 1.256 | 1.038 | 1.239 | 1.297 | $< 39$ [41] |
| $\overline{B}^0\to \overline{K}^0\omega$ | 0.034 | 0.083 | 0.007 | 0.026 | 0.076 | 0.012 | see Tab.III |
| $\overline{B}^0\to \overline{K}^0\phi$ | 3.663 | 5.945 | 6.703 | 3.589 | 5.833 | 6.569 | see Tab.III |
| $\overline{B}^0\to \pi^+K^{*-}$ | 1.838 | 2.411 | 2.743 | 3.281 | 4.077 | 4.36 | see Tab.III |
| $\overline{B}^0\to \pi^0\overline{K}^{*0}$ | 0.533 | 0.744 | 0.896 | 0.459 | 0.714 | 0.875 | $< 3.6$ [15] |
| $\overline{B}^0\to \eta\overline{K}^{*0}$ | 2.072 | 2.681 | 2.972 | 2.15 | 2.67 | 2.927 | see Tab.III |
| $\overline{B}^0\to \eta'\overline{K}^{*0}$ | 0.759 | 1.717 | 1.891 | 0.689 | 1.662 | 1.84 | $< 24$ [13] |
| $B^-\to \pi^-\overline{K}^{*0}$ | 2.583 | 3.497 | 3.814 | 2.531 | 3.433 | 3.731 | see Tab.III |
| $B^-\to \pi^0K^{*-}$ | 1.852 | 2.317 | 2.489 | 3.067 | 3.543 | 3.667 | $< 31$ [15] |
| $B^-\to \eta K^{*-}$ | 1.777 | 2.247 | 2.591 | 2.564 | 3.022 | 3.306 | see Tab.III |
| $B^-\to \eta' K^{*-}$ | 1.446 | 2.664 | 2.83 | 1.046 | 2.091 | 2.277 | $< 35$ [13] |
| $B^-\to \overline{K}^0\rho^-$ | 0.403 | 0.598 | 0.789 | 0.395 | 0.585 | 0.777 | $< 48$ [41] |
| $B^-\to K^-\rho^0$ | 0.453 | 0.426 | 0.528 | 0.609 | 0.503 | 0.631 | see Tab.III |
| $B^-\to K^-\omega$ | 0.583 | 0.530 | 0.435 | 0.580 | 0.565 | 0.495 | see Tab.III |
| $B^-\to K^-\phi$ | 3.911 | 6.346 | 7.179 | 3.831 | 6.227 | 7.02 | see Tab.III |

TABLE VI. CP-violating asymmetry parameters $a_{\epsilon'}$, and $a_{\epsilon+\epsilon'}$ (in units of $10^{-2}$) for decays $\overline{B}^0 \to PV$ with central values of various parameters within the QCDF framework. The results in columns 2∼5 are calculated with $A = 0.819$, $\lambda = 0.2237$, $\bar{\rho} = 0.218$, and $\bar{\eta} = 0.316$, while the results in columns 6∼9 are calculated with $A = 0.83$, $\lambda = 0.222$, $\bar{\rho} = 0.05$, and $\bar{\eta} = 0.381$.

| modes | $a^f_{\epsilon'}$ | $a^{f+a}_{\epsilon'}$ | $a^f_{\epsilon+\epsilon'}$ | $a^{f+a}_{\epsilon+\epsilon'}$ | $a^f_{\epsilon'}$ | $a^{f+a}_{\epsilon'}$ | $a^f_{\epsilon+\epsilon'}$ | $a^{f+a}_{\epsilon+\epsilon'}$ |
|---|---|---|---|---|---|---|---|---|
| $\pi^0\rho^0$ | -11.11 | -6.90 | 48.29 | 51.66 | -14.01 | -8.88 | -39.15 | -34.80 |
| $\pi^0\omega$ | 19.08 | 80.95 | 94.80 | 32.56 | 28.82 | 80.02 | 95.35 | 10.70 |
| $\eta\rho^0$ | 31.78 | 16.77 | -17.31 | 10.53 | 28.11 | 17.11 | -87.88 | -75.06 |
| $\eta'\rho^0$ | -28.02 | -34.78 | 89.23 | 92.18 | -39.96 | -54.92 | 88.09 | 66.99 |
| $\eta\omega$ | 44.82 | 29.66 | 74.53 | 81.05 | 64.64 | 45.06 | 16.02 | 26.05 |
| $\eta'\omega$ | -20.57 | -16.88 | 32.27 | 26.95 | -23.60 | -18.81 | -56.70 | -62.16 |
| $K^0_S\rho^0$ | -5.56 | -8.92 | 64.39 | 66.25 | -6.27 | -10.20 | 62.38 | 64.40 |
| $K^0_S\omega$ | -41.77 | 86.90 | 79.28 | -48.78 | -54.10 | 62.18 | 73.15 | -61.69 |
| $K^0_S\phi$ | -0.99 | -0.97 | 73.24 | 73.40 | -1.19 | -1.17 | 72.91 | 73.11 |
| $\pi^0\phi$ | 0 | — | 2.29 | — | 0 | — | 1.83 | — |
| $\eta^{(\prime)}\phi$ | 0 | 0 | 2.29 | 2.29 | 0 | 0 | 1.83 | 1.83 |

TABLE VII. CP-violating asymmetries $\mathcal{A}_{CP}$ (%) for $B\to PV$ ($b\to d$ transitions) with central values of various parameters within the QCDF approach. The results in the 2nd and 3rd columns are calculated with $A = 0.819$, $\lambda = 0.2237$, $\bar{\rho} = 0.218$, and $\bar{\eta} = 0.316$, while the results in the 4th and 5th columns are computed with $A = 0.83$, $\lambda = 0.222$, $\bar{\rho} = 0.05$, and $\bar{\eta} = 0.381$.

| modes | $\mathcal{A}_{CP}^{f}$ | $\mathcal{A}_{CP}^{f+a}$ | $\mathcal{A}_{CP}^{f}$ | $\mathcal{A}_{CP}^{f+a}$ |
|---|---|---|---|---|
| $B^0\to K_S^0\overline{K}^{*0}$ | 22.38 | 23.89 | 19.60 | 20.37 |
| $B^0\to K_S^0 K^{*0}$ | -11.34 | -11.97 | -9.14 | -9.36 |
| $B^0\to K^{\pm}K^{*\mp}$ | — | 17.41 | — | -25.49 |
| $B^0\to\pi^-\rho^+$ | 17.09 | 20.16 | -13.47 | -9.60 |
| $B^0\to\pi^+\rho^-$ | 25.64 | 21.51 | -26.91 | -31.85 |
| $\overline{B}^0\to\pi^0\rho^0$ | 15.75 | 20.10 | -27.78 | -22.36 |
| $\overline{B}^0\to\pi^0\omega$ | 57.59 | 68.32 | 64.21 | 57.29 |
| $\overline{B}^0\to\eta\rho^0$ | 12.49 | 15.95 | -23.52 | -24.58 |
| $\overline{B}^0\to\eta'\rho^0$ | 24.21 | 21.21 | 15.88 | -3.92 |
| $\overline{B}^0\to\eta\omega$ | 64.74 | 57.95 | 49.80 | 41.81 |
| $\overline{B}^0\to\eta'\omega$ | 1.95 | 1.83 | -42.40 | -41.88 |
| $\overline{B}^0\to\pi^0\phi$ | 1.09 | — | 0.87 | — |
| $\overline{B}^0\to\eta^{(\prime)}\phi$ | 1.09 | 1.09 | 0.87 | 0.87 |
| $B^-\to\pi^-\rho^0$ | 3.26 | 12.47 | 3.58 | 13.76 |
| $B^-\to\pi^-\omega$ | -6.22 | -6.64 | -8.18 | -8.73 |
| $B^-\to\pi^-\phi$ | 0 | — | 0 | — |
| $B^-\to\pi^0\rho^-$ | -2.98 | -9.09 | -4.0 | -12.14 |
| $B^-\to\eta\rho^-$ | -1.75 | -2.05 | -2.21 | -2.59 |
| $B^-\to\eta'\rho^-$ | 5.03 | 4.94 | 5.85 | 5.74 |
| $B^-\to K_S^0 K^{*-}$ | -8.82 | 8.94 | -6.94 | 7.83 |
| $B^-\to K^-K^{*0}$ | -25.28 | -33.23 | -21.78 | -26.58 |

TABLE VIII. CP-violating asymmetries $\mathcal{A}_{CP}$ (%) for $B\to PV$ ($b\to s$ transitions) with central values of various parameters within the QCDF approach. The results in the 2nd and 3rd columns are calculated with $A = 0.819$, $\lambda = 0.2237$, $\bar{\rho} = 0.218$, and $\bar{\eta} = 0.316$, while the results in the 4th and 5th columns are computed with $A = 0.83$, $\lambda = 0.222$, $\bar{\rho} = 0.05$, and $\bar{\eta} = 0.381$.

| modes | $\mathcal{A}_{CP}^{f}$ | $\mathcal{A}_{CP}^{f+a}$ | $\mathcal{A}_{CP}^{f}$ | $\mathcal{A}_{CP}^{f+a}$ |
|---|---|---|---|---|
| $\overline{B}^0\to K^-\rho^+$ | 1.62 | -34.31 | 2.68 | -54.21 |
| $\overline{B}^0\to K_S^0\rho^0$ | 27.04 | 25.73 | 25.62 | 24.01 |
| $\overline{B}^0\to K_S^0\omega$ | 10.51 | 33.46 | -0.46 | 11.19 |
| $\overline{B}^0\to K_S^0\phi$ | 34.23 | 34.32 | 33.95 | 34.05 |
| $\overline{B}^0\to \pi^+K^{*-}$ | 20.57 | 47.0 | 14.36 | 34.92 |
| $\overline{B}^0\to \pi^0\overline{K}^{*0}$ | -9.49 | -9.51 | -11.69 | -11.50 |
| $\overline{B}^0\to \eta\overline{K}^{*0}$ | 5.05 | 5.52 | 5.99 | 6.61 |
| $\overline{B}^0\to \eta'\overline{K}^{*0}$ | -5.51 | -5.56 | -6.72 | -6.75 |
| $B^-\to \pi^-\overline{K}^{*0}$ | 0.97 | 1.23 | 1.17 | 1.49 |
| $B^-\to \pi^0K^{*-}$ | 18.86 | 35.57 | 14.56 | 28.51 |
| $B^-\to \eta K^{*-}$ | 7.73 | 29.28 | 6.79 | 27.09 |
| $B^-\to \eta' K^{*-}$ | -13.78 | -20.39 | -20.73 | -29.92 |
| $B^-\to K_S^0\rho^-$ | 0.31 | -0.34 | 0.38 | -0.41 |
| $B^-\to K^-\rho^0$ | 2.88 | -80.25 | 2.87 | -79.31 |
| $B^-\to K^-\omega$ | 59.85 | -19.92 | 66.26 | -20.63 |
| $B^-\to K^-\phi$ | 0.99 | 1.17 | 1.19 | 1.41 |